UNIVERSITY OF CALIFORNIA,
IRVINE

Heat Transfer Model for Hot Air Balloons
THESIS

submitted in partial satisfaction of the requirements
for the degree of

MASTER OF SCIENCE

in Mechanical and Aerospace Engineering

by

Adriana Lladó-Gambín

Thesis Committee:
Professor Derek Dunn-Rankin, Chair
Professor Manuel Gamero Castaño
Professor Jaeho Lee

2016

TABLE OF CONTENTS

LIST OF FIGURES

LIST OF TABLES

ACKNOWLEDGMENTS

I would like to express the deepest gratitude to my advisor Professor Dunn-Rankin for all his support. I feel very lucky to have had the chance to work under his guidance. His continuous encouragement and our discussions are very valuable to me, and without him none of this would have been possible.

I also thank Ultramagic for their collaboration as a hot air balloon manufacturer. They provided very useful information.

ABSTRACT OF THE THESIS

Heat Transfer Model for Hot Air Balloons

By

Adriana Lladó-Gambín

Master of Science in Mechanical and Aerospace Engineering

University of California, Irvine, 2016

Professor Derek Dunn-Rankin

A heat transfer model and analysis for hot air balloons is presented in this work, backed with a flow simulation using SolidWorks. The objective is to understand the major heat losses in the balloon and to identify the parameters that affect most its flight performance. Results show that more than 70% of the heat losses are due to the emitted radiation from the balloon envelope and that convection losses represent around 20% of the total. A simulated heating source is also included in the modeling based on typical thermal input from a balloon propane burner. The burner duty cycle to keep a constant altitude can vary from 10% to 28% depending on the atmospheric conditions, and the ambient temperature is the parameter that most affects the total thermal input needed. The simulation and analysis also predict that the gas temperature inside the balloon decreases at a rate of $-0.25\ K/s$ when there is no burner activity, and it increases at a rate of $+1\ K/s$ when the balloon pilot operates the burner. The results were compared to actual flight data and they show very good agreement indicating that the major physical processes responsible for balloon performance aloft are accurately captured in the simulation.

INTRODUCTION

This work presents a heat transfer model for hot air balloons. Developing a thermal model for a balloon is not new, but this study comprehensively refines past approaches and includes a flow simulation to compare with the analytical results in order to provide more insight on the gas temperature distribution inside the balloon envelope. The distribution is a potentially important aspect to include because non-uniform heating of the fabric can lead to its early degradation.

There have been a few trajectory and thermal models for gas balloons developed because of their scientific use at high altitude. Kreith published several studies in the 1970s, including a numerical prediction of the performance [1] and an energy balance [2]. Later, Carlson and Horn developed another thermal and trajectory model, also for high-altitude balloons [3].

For hot air balloons the extent of the literature is emore limited. Stefan provided the first thermal and performance model for hot air balloons in 1979 [4]. He identified the energy factors affecting the balloon, evaluated all the parameters present in the equations, and compared his results with real flight data to adjust the convection coefficients which are otherwise difficult to assess. In 1991 there was an international symposium for Hot Air Aerostatic Vehicle Technology, which included a suite of different studies from Hallmann and Herrmann, from Aachen University. These were the first publications with experimental data. Based on this data, they reported a slightly different heat transfer model [5], supported by an experimentally determined temperature profile

[6] and measurements of velocity distribution and gas composition by Röder et al. [7]. Hallmann and Herrmann also tested the porosity and strength behavior of hot air balloon fabrics subject to temperature load, and discussed their radiation properties [8]. These few studies are the only ones that have found their way into the open literature. While their methodology is globally sound, they have not incorporated some of the modern elements of hot air balloons and they have not taken advantage of advances in flow simulation. The refinement and expansion of these earlier models, along with a companion study using simulation is the goal of this thesis.

The thesis is divided into two main parts. The first part describes the heat transfer model, which is an update and refinement of older models which includes a new way to estimate the air entrained by the flame [9] and new convection coefficient correlations from more recent studies [10][11]. The second part is the flow simulation using a real balloon envelope geometry and Solidworks finite element modeling software. It is a time dependent study that simulates the burner operation by activating a heat source in order to verify the analytical results of burner operation time. Results from the simulation are compared to real flight data of temperature [6] and velocity. The overall objective of this work is to understand the major thermal losses in the balloon and the parameters that affect those losses most significantly.

1. HOT AIR BALLOON CHARACTERISTICS

There are three main parts in a hot air balloon: envelope, burner and basket.

The **envelope** (shown in Figure 1) is composed of many gores (the large vertical sections that are stitched together into the balloon envelope) made of a high resistance Nylon fabric, reinforced by several polyester load tapes. These load tapes transmit the loading forces via stainless steel cables to the load frame. In the top of the envelope there is a large hole, where there is no fabric but the mesh of load tapes continues. The hole is covered from the inside of the balloon by a loose panel of fabric called parachute. It is kept closed by the internal pressure of the gas in the balloon and it is opened from the basket by pulling a cord in a completely reversible process.

The volume of the envelope can range from 1,200 to 12,000 m^3. The specific balloon chosen for this study is an Ultramagic M-77, with a volume of 2,200 m^3, but the results obtained are fairly independent of balloon specifics. Furthermore, the M-77 is representative of the most common size for ballooning competition and advertisement.

The **basket** (shown in Figure 2) is made from woven willow and cane in a marine plywood base. It is connected to the load frame by stainless steel cables that pass down the sides and through and under the base. The standard basket for a 2,200 m^3 balloon weights 56 kg.

Figure 1. Hot air balloon, model MV-77

Figure 2. Hot air balloon basket, model C-1 (standard for 2,200 m3 size balloon)

The **burner** (shown in Figure 3) converts the fuel (liquid propane) stored in the fuel cylinders into heat energy. This energy is used to heat the air inside the balloon envelope and thus provide the means of inflation and altitude control during flight. The burner has two different valves through which the propane can flow. The main or blast valve allows fuel to pass through a coil to be pre-heated so that it burns in gas phase at the jet's ring outlets. This valve of the burner gives the maximum power. The liquid fire or quiet burner valve feeds fuel directly to the multi hole jet assembly without passing it through the coil. The liquid fuel mode is less efficient but the flame is quieter for use when flying near animals. The ignition of the fuel in both cases is provided by a continuous pilot flame, fitted with a shutoff valve and piezoelectric igniter.

This study considers for specificity the MK-32 burner model from Ultramagic, with a maximum power of 3.2 MW at a nominal pressure of 6 bar. The jet's ring has 40 holes of 1.35 mm diameter each.

The air intakes highlighted in Figure 3 allow air to flow into the burner for the correct combustion of fuel. In addition, they reduce the weight of the can. Figure 4 shows the burner in operation during inflation.

Figure 3. Ultramagic MK-32 single burner

Figure 4. Burner in operation during inflation

The fuel flow rate was measured for both the main flame and the pilot flame using a high precision scale. For the main flame (fuel burning at gas phase under maximum burn conditions) the obtained flow rate was $\dot{m}_b = 67.8\, gr/s$, and for the pilot flame $\dot{m}_p = 0.07\, gr/s$. Even recognizing that the pilot flame is on continuously and the burner is used in bursts (duty cycle of perhaps 10%-25%) it is clear that the fuel used to keep the pilot flame alive is negligible (i.e., less than 1%). Assuming 50 kJ/g heat of combustion for propane, the main burner flow rate is equivalent to 3.04 MW, which is close to the manufacturer's nominal stated value for the burner.

Figure 5 shows the measured emissions using Enerac 700 combustion analyzer and Figure 6 the flue temperature for the pilot flame:

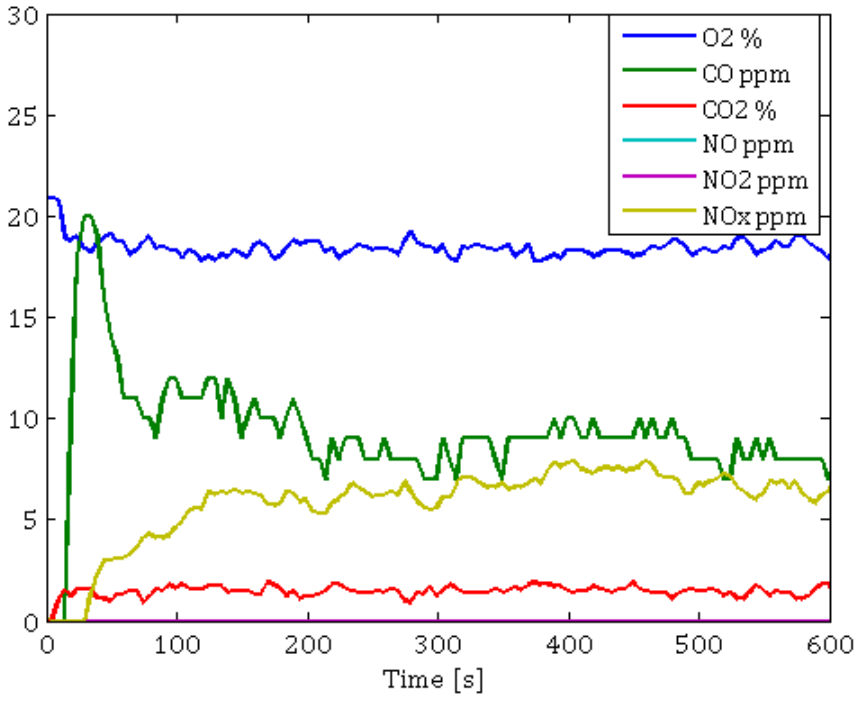

Figure 5. Data from Enerac 700 combustion analyzer for the pilot flame

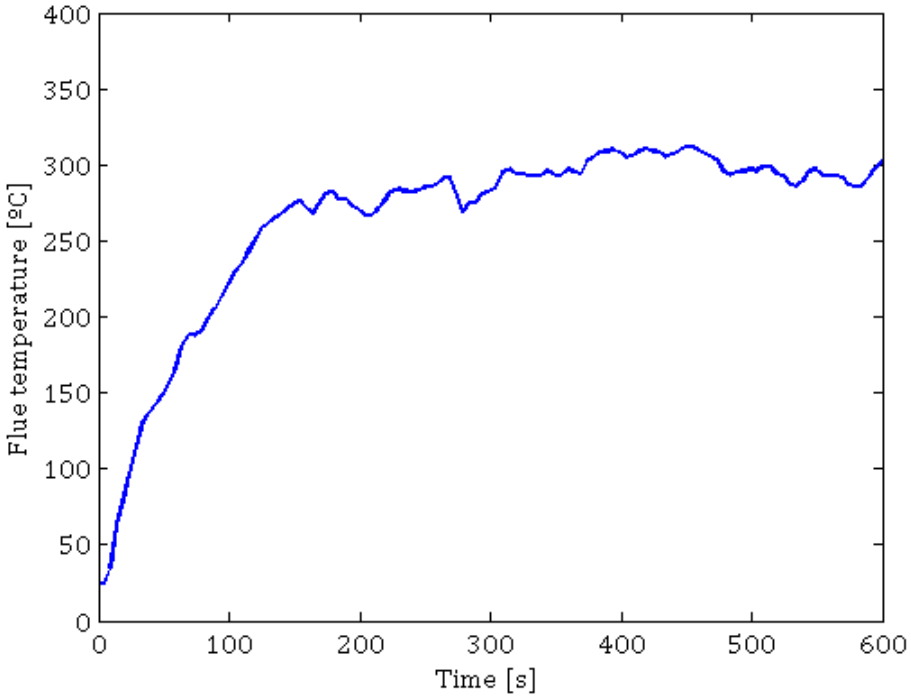

Figure 6. Measured flue temperature for the pilot flame

The flue temperature reaches a constant value of approximately 270 ℃ at $t = 150s$. Table 1 shows the average concentration for every measured parameter from $t = 150s$ to $t = 600s$:

CO	8.53 ppm
CO2	1.49 %
O2	18.35 %
NO	6.82 ppm
NO2	0
HxCy	0

Table 1. Average measured concentrations for the pilot flame

Using British Standard BS845 norm [12] we can calculate the combustion efficiency. The heat lost by incomplete combustion of the fuel is:

$$Q_{losses} = k\frac{[CO] + [H_xC_y]}{[CO_2] + [CO] + [H_xC_y]} \quad (1)$$

Where $k = 81.8$ for pure propane. The concentration of hydrocarbons has been measured to be zero. Then the efficiency is:

$$\eta = \frac{Q_{C_3H_8} - Q_{losses}}{Q_{C_3H_8}} \quad (2)$$

Where $Q_{C_3H_8} = 46.28\ MJ/kg$ is the low heating value for propane. We get an efficiency for the pilot flame of 99.99%.

Fabric properties

For Nylon the maximum continuous acceptable operating temperature is 100°C, and it should never exceed 125°C.

The fabric weight is approximately 65 gr/m^2, its thickness 0.1 mm, and its thermal conductivity can vary from 0.003 to 0.04 W/mK depending on the fabric color and the temperature [8].

As for the radiation properties, the ratio absorptivity/emissivity is critical for the energy balance and the thermal behavior on the fabric surface. Forty surfaces of hot air balloon fabric were examined at the FH Aachen [8], and the results show that the emissivity for most colors is between 0.86 and 0.88, while for silver it is 0.70. The absorptivity α is about 0.5 for light colors to 0.9 for dark colors. For the inner surface the emissivity ranges from 0.85 to 0.88. The values above show that a fairly dramatic

thermal modification effect may be achieved with silver fabric, and some manufacturers have developed balloons with such fabric for high-efficiency flying.

What we want is a material with a large $\alpha/\varepsilon > 1$ and a small emissivity to minimize consumption. All fabrics, except the silver one, have a high emission coefficient, but the absorption is less with bright colors.

The fabric porosity has been proved to be completely negligible for the first 200 hours, and after that porosity increases slowly but exponentially [8]. Too much porosity means the fabric is fatigued, so it can be used to characterize the envelope lifetime.

1. HEAT TRANSFER MODEL

The motion of a hot air balloon depends on the heat transfer to and from the gas inside, since the temperature of the gas determines the lift of the balloon. This section presents an energy balance and heat transfer model that includes all heat losses.

Figure 7 shows the heat transfer modes involved in the total energy balance.

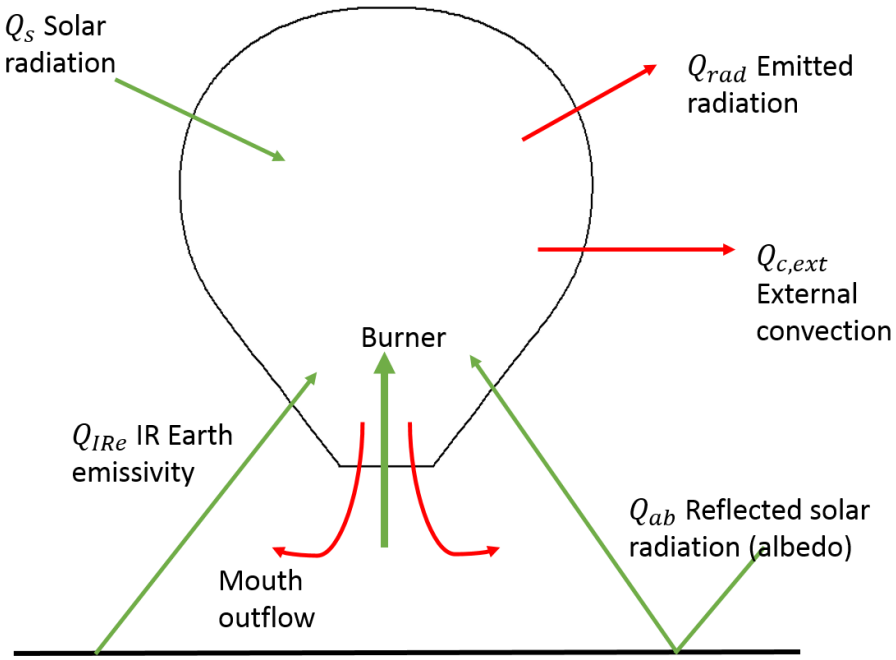

Figure 7. Heat transfer modes in a hot air balloon

The radiation heat that the envelope absorbs from the environment consists of the solar radiation, direct and reflected, and the infrared radiation emitted by the Earth's surface.

The heat transfer between the contained gas and the envelope is mostly by internal convection and some radiation.

Finally, we need to include in our balance the losses and the burner input. The losses include the envelope's emitted radiation, external convection to the ambient air and what we call the mouth outflow. The latter occurs when the burner is active and exhaust gases (mostly air) are introduced to the envelope. This leads to an overflow of warm internal gases that carry away an amount of sensible heat.

Direct solar radiation

$$Q_S = F_S \alpha \frac{A}{4} \tag{3}$$

F_S is the solar flux, which varies from 0 to a maximum of about 1260 W/m^2, and α is the envelope absorptivity, which is about 0.5 for light colors to 0.9 for dark colors (as described earlier). The effective receiving area is the projected area $A/4$.

Reflected solar radiation

$$\boldsymbol{Q_S = F_S d \alpha \frac{A}{4}} \tag{4}$$

d is the proportion of solar flux reflected by the Earth or clouds (albedo). It is roughly 0.1 over most surfaces, 0.3 over desert, 0.8 over snow or ice and 0.55 over clouds. Since the reflection is generally diffuse, it acts on an effective area of $A/2$.

Earth IR radiation

$$Q_{IRe} = \varepsilon_e \varepsilon \tau_a \sigma \frac{A}{2} T_e^4 \tag{5}$$

ε_e is the Earth's surface emissivity, which is usually assumed to be between 0.8 and 1 [13], τ_a is the atmospheric transmissivity, and T_e is the Earth's surface temperature (assumed to be the same as the ambient temperature). τ_a varies from 0 to 1 depending on altitude and atmospheric conditions. A value of 0.6 to 0.7 is commonly used for clear sky atmospheric transmission [14].

Emitted radiation

$$Q_{rad} = \varepsilon \sigma A T_s^4 \tag{6}$$

Where T_s is the envelope (skin) temperature and ε the envelope emissivity.

External and internal convection heat transfer

$$Q_{c,ext} = h_{ext} A (T_s - T_a) \tag{7}$$

The convection coefficient varies with temperature, velocity, density, and balloon size. The similarity parameters for natural convection are the Prandtl number *Pr*, which represents the ratio between momentum diffusivity and thermal diffusivity, and the Grashof number *Gr*, which represents the ratio of buoyant to viscous forces. The Grashof number and the Prandtl number are often grouped together as a product GrPr, which is called the Rayleigh number, Ra.

$$Pr = \frac{C_p \mu}{k} \tag{8}$$

$$Gr = \frac{g\beta(T_s - T_\infty)L^3}{\nu^2} \tag{9}$$

L is the length scale, which in this case is the diameter at the equator $D = 16.67\ m$. C_p, μ, k, β and ν are the specific heat capacity, the dynamic viscosity, the thermal conductivity, the coefficient of thermal expansion, and the kinematic viscosity of air. All properties are evaluated at the film temperature:

$$T_f = \frac{(T_s + T_\infty)}{2} \tag{10}$$

Plugging all the numbers into the equations yields $Pr = 0.708$ and $Gr = 7.2 \cdot 10^{12}$. The Rayleigh number is then $Ra = PrGr = 5.1 \cdot 10^{12}$. Several correlations are available from the literature, but few for such large Rayleigh number.

For external convection [10] and [15] recommend Campo's correlation [11]:

$$Nu = 0.1Ra^{0.340} \qquad Ra \geq 1.5 \cdot 10^8 \tag{11}$$

Which gives a Nusselt number of $Nu = 2092$ and an external convection coefficient of $h = k \cdot Nu/D = 3.37\ W/m^2K$.

Internal convection heat transfer

$$Q_{c,int} = h_{int} A\left(T_g - T_s\right) \tag{12}$$

For the internal convection coefficient, the temperature difference in the Grashof number is the difference between the internal gas temperature T_g and the envelope temperature T_s. This gives a Rayleigh number of $Ra = 2.28 \cdot 10^{13}$.

Carlson and Horn [3] use

$$Nu = 0.325 \cdot Ra^{0.333} \qquad Ra \geq 1.35 \cdot 10^8 \tag{13}$$

Which gives a Nusselt number of $Nu = 9122$ and an internal convection coefficient of $h = 16\, W/m^2K$. Both correlations are developed for the situation of convection around a sphere at uniform temperature.

Radiation gas-envelope

$$Q_r = Q_{g \to s} = \sigma A f\left(T_g^4 - T_s^4\right) \tag{14}$$

$$f = \frac{1}{\frac{1-\varepsilon_g}{\varepsilon_g} + 1 + \frac{A_1}{A_2}\frac{1-\varepsilon_{in}}{\varepsilon_{in}}} \tag{15}$$

The equations above are for the net radiation between concentric spheres and the view factor [2]. It can also be used for a gas and its enclosure with $A_1 = A_2 = A$. The emissivity of the mixture of gases in the atmosphere is $\varepsilon_a = 0.31$. The gas emissivity for the air inside the balloon will not differ too much. Also, the radiation exchange is almost negligible (see chapter 0), so a change in this parameter does not significantly affect the

overall heat transfer balance. ε_{in} is the emissivity of the envelope's inner surface (see chapter 1).

Mouth outflow loss

$$Q_o = \dot{m}_{out} c_p (T_g - T_a) \tag{16}$$

c_p is the air heat capacity. It is actually a mix of air and combustion products, but it is generally assumed that there is only hot air since entrainment is very high. This is not a bad assumption, and the errors produced are something less than 2% [4].

The flow rate $\dot{m}_{out}$ is the mass introduced by the burner since we are assuming $m_{in} = m_{out}$ for a whole period. The balloon takes the increase in mass for the short time that the burner is operation, and then steadies later with the mass leaving slowly. In terms of calculation, we do not care about actual outflow rate since the balloon acts as a thermal energy capacitor; we just care about the total outflow in one cycle (from the beginning of a burst until right after the following one). Therefore we can write $\dot{m}_{in} = \dot{m}_{out}$ and approximate $E_{outflow} = kQ_{outflow}$, where k is the burner duty cycle. The inflow includes the fuel flow and the air entrained by the flame. It has been calculated following the procedure described by Becker for vertical free turbulent diffusion flames [9]:

$$\xi < 1 \qquad \dot{m} = \frac{0.16\dot{m}_0}{D_s} x \tag{17}$$

$$1 < \xi < 2.5 \qquad \dot{m} = \frac{\dot{m}_0}{D_s}\left(0.0056 \cdot Ax^4 + 0.026A^{\frac{1}{2}}x^{\frac{5}{2}} + 0.13x\right) \tag{18}$$

$$\xi > 2.5 \qquad \dot{m} = \frac{\dot{m}_0}{D_s}\left(0.082A^{\frac{1}{2}}x^{5/2} - 0.0068x\right) \tag{19}$$

$\dot{m}_0 = 67.8\ gr/s$ is the measured fuel flow (see chapter 1) and D_s is the effective source diameter. The expressions above show the flow rate distribution at three different regimes: forced convection $\xi < 1$, transition regime $1 < \xi < 2.5$ and natural convection regime $\xi > 2.5$. The parameter ξ is defined as follows:

$$\xi = \left(\frac{\pi g \rho_\infty}{4\dot{G}_0}\right)^{1/3} x \tag{20}$$

Where $\dot{G}_0$ is the jet momentum flux at the burner exit $\dot{G}_0 = U_s \cdot \dot{m}_0$, so $\dot{m} = f(x, \dot{m}_0, D_s, U_s, \rho_\infty)$.

The effective source diameter is the throat diameter of an imagined flow nozzle from which fluid of density ρ_∞ issues at mass rate $\dot{m}_0$, momentum rate $\dot{G}_0$, and uniform exit velocity $U_s = \dot{G}_0/\dot{m}_0$. For a multiport array where port-exit distributions of density and velocity are considered uniform:

$$D_s = \left(\frac{4A_s}{\pi}\right)^{1/2} \left(\frac{\rho_0}{\rho_\infty}\right)^{1/2}; \quad A_s = \sum \frac{\pi D_i^2}{4} \tag{21}$$

The burner under study (Ultramagic MK-32) has 40 jets with a diameter of $1.35mm$ each. With $\rho_\infty = 1.225\ kg/m^3$ and initial fuel density $\rho_0 = 15.808\ kg/m^3$ we get a source diameter of $D_s = 30.67\ mm$.

In order to know the flow rate at the mouth envelope, we need to calculate at which distance the transition from one regime to another one occurs. First of all the jet exit velocity is needed to get the momentum flux at the burner exit. For a converging tube, we have choked flow when $P/P_0 \leq 0.528$, where P is the pressure in the fuel cylinder and P_0 the ambient pressure. The pressure in the cylinder can go from 3 to 10 bar, so the

nozzle is always choked. This means the flow is moving at Mach 1 at the exit. For an ideal gas we have:

$$U_s = \sqrt{\frac{\gamma RT}{M}} \tag{22}$$

Where $\gamma = 1.247$ is the specific heat ratio for propane, $M = 44.1\ g/mol$ is the molar mass and T is the exit temperature, assumed to be equal to the ambient temperature. By solving the equation we find that $U_s = 260.5\ m/s$.

Now using equations 17, 18, and 19 we can plot the mass flow rate as a function of the flame length x:

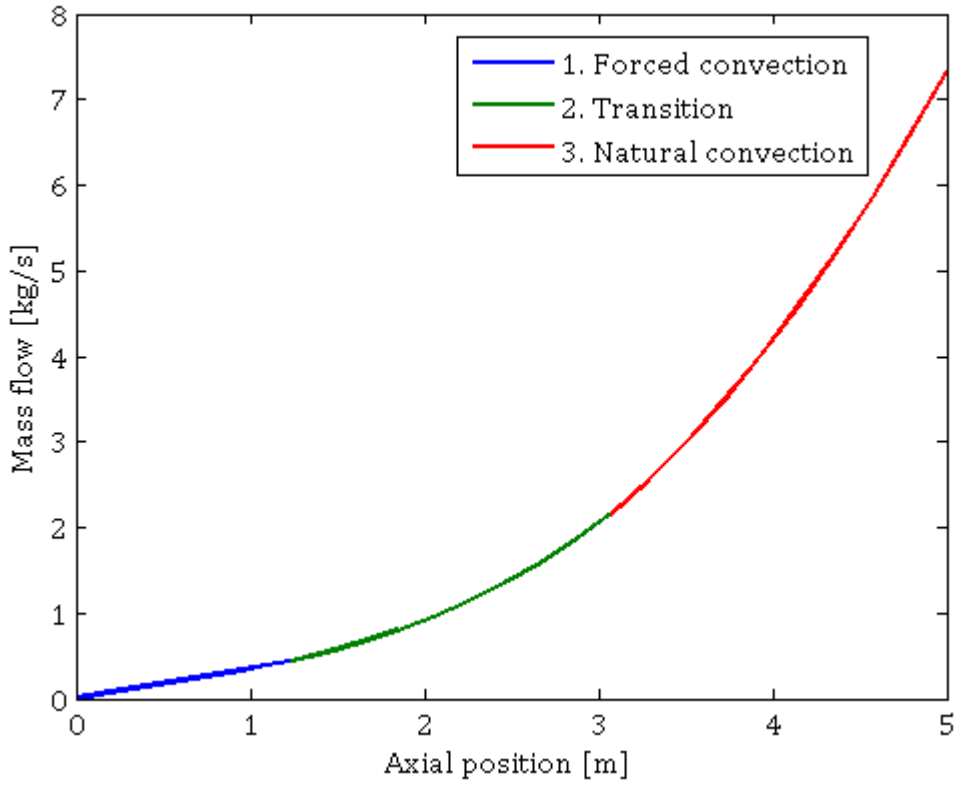

Figure 8. Air entrainment vs distance from the burner exit

The mouth of the envelope is at a distance of 2.47 m from the burner exit, where the mass flow rate is $\dot{m} = 1.356\ kg/s$. The heat losses from the outflow generated can now be determined with equation 16.

2. PERFORMANCE

The intention of this section is to show the calculation of performance aspects within the balloon. First we introduce the forces acting on the body: lift, drag and weight.

Lift L

From the principle of Archimedes, we have:

$$L = Vg(\rho_a - \rho_g) \tag{23}$$

Where V is the volume of the envelope and ρ_a, ρ_g are the ambient air density and the gas density respectively. Assuming the gases to be ideal:

$$L = Vg\left(\frac{P_a}{R_a T_a} - \frac{P_g}{R_g T_g}\right) \tag{24}$$

We assumed there is only hot air inside the envelope, so we have that $R_g = R_a$. The equation can be further reduced assuming there is no difference in pressures so $P_g = P_a$. Rearranging equation 24 we find:

$$L = Vg\rho_a(1 - T_a/T_g) \tag{25}$$

So the lift is only a function of the gas volume, the ambient density and temperature, and the gas temperature.

Drag D

The drag force is defined as follows:

$$D = \frac{1}{2} C_d \rho_a u^2 S \tag{26}$$

Where C_d is the drag coefficient and $S = \pi R^2$ the cross-sectional area in the equator where the radius is maximum $R = 16.67/2\, m$. From [4] we know that wind tunnel measurements for a balloon in vertical motion give a value of about 0.4 for the drag coefficient.

Gross weight G

The gross weight includes the balloon weight (envelope, burner, basket and cylinders) and the payload.

Neutral buoyancy

When the balloon is at neutral buoyancy (hovering) there is no vertical speed and we can say that:

$$L - G = 0 \tag{27}$$

Substituting the expression for the lift we find:

$$T_g = \frac{T_a}{\left(1 - \frac{G}{V \rho_a g}\right)} \tag{28}$$

Since the ambient temperature and density are just a function of the altitude, we can obtain the necessary gas temperature needed to lift a weight G at any altitude.

Within the troposphere ($h < 11000\ m$), the ISA temperature and density depend on the altitude as follows:

$$T = T_0 - 0.0065h \tag{29}$$

$$\rho = \rho_0 \left(1 - 0.0065 \frac{h}{T_0}\right)^{4.2561} \tag{30}$$

Where $T_0 = 288.15\ K$ and $\rho_0 = 1.225\ kg/m^3$ are the sea level conditions.

With that, we can obtain different plots for a gas volume of $V = 2200\ m^3$, which corresponds to the Ultramagic M-77 model. Figure 9 shows the gross weight as a function of the altitude for a gas temperature of 373 K, which is the maximum continuous temperature that the Nylon fabric can handle.

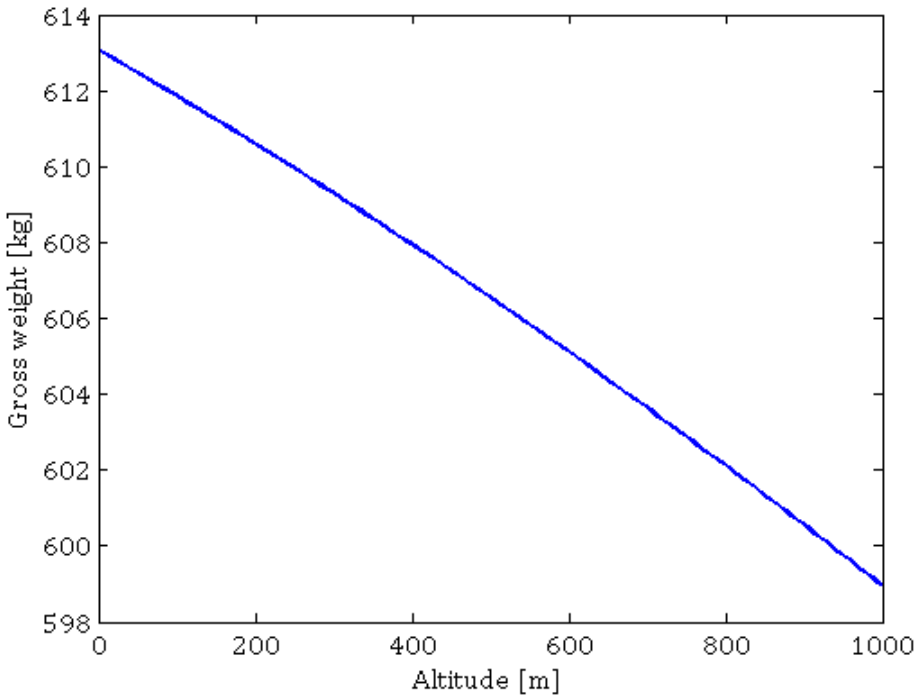

Figure 9. Gross weight vs altitude for an ambient temperature of 288 K and a gas temperature of 373 K

It is interesting to see that the temperature gradient $\Delta T = T_{gas} - T_{ambient}$ increases with increasing ambient temperature (Figure 10), for a fixed altitude (SL) and gross weight ($613\ kg$).

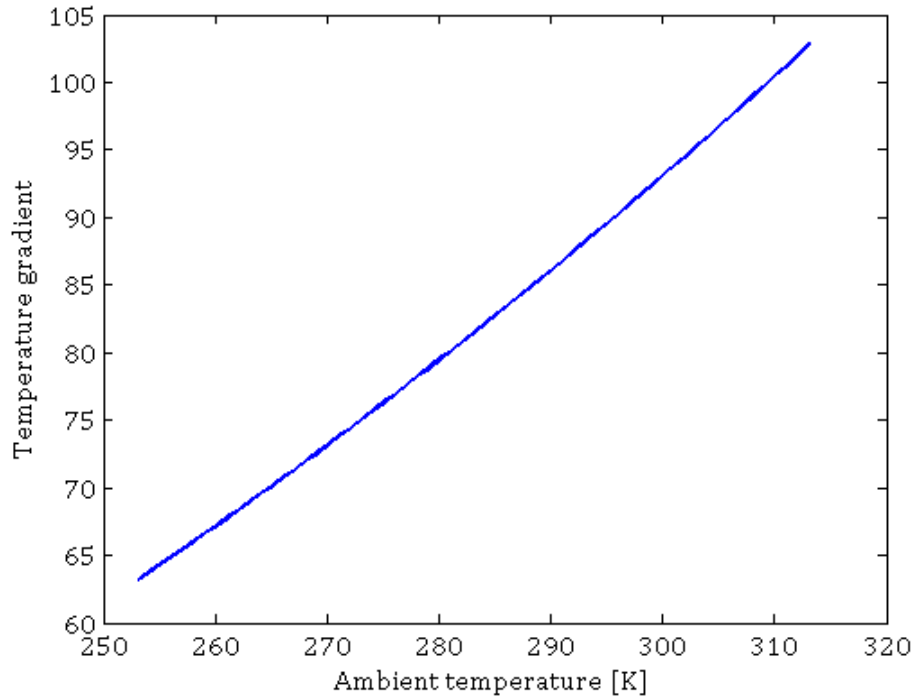

Figure 10. Temperature gradient Tgas-Tambient vs ambient temperature for a gross weight of 613 kg at sea level

And, as shown in Figure 11, for a lower load the internal temperature is going to be lower.

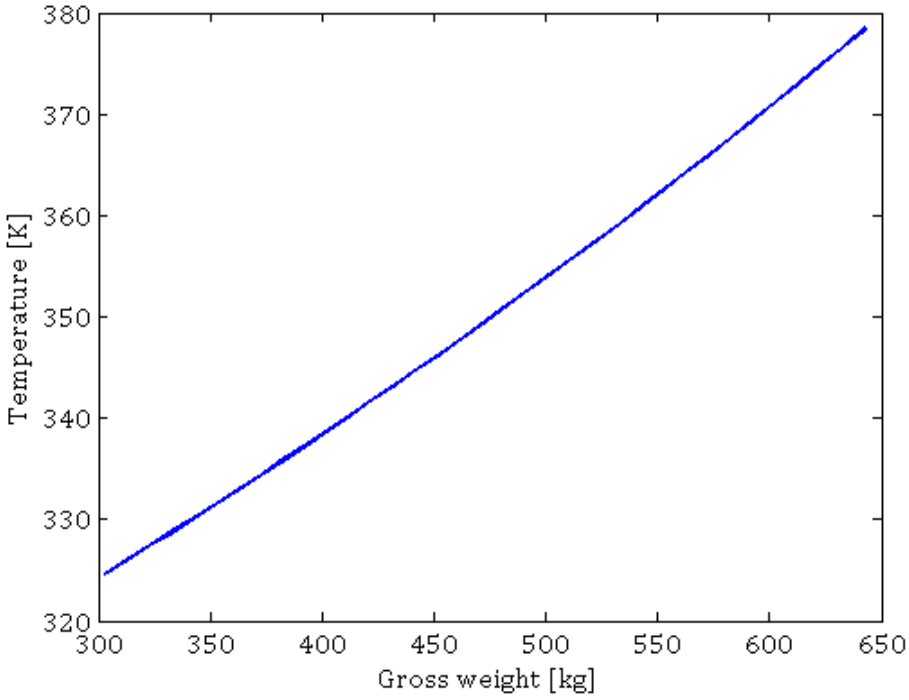

Figure 11. Gas temperature vs weight for an ambient temperature of 288 K at SL

Vertical motion

The equation for vertical motion is:

$$L - G + D = m\frac{dv}{dt} = \left(V\rho_g + \frac{G}{g}\right)\frac{dv}{dt} \tag{31}$$

Assuming that T_a and ρ_a are constant, and that the drag coefficient is constant too, we have that the acceleration is:

$$\frac{du}{dt} = -\frac{1}{\left(V\rho_a\left(T_a/T_g(t)\right) + \frac{G}{g}\right)}\left(Vg\rho_a\left(1 - T_a/T_g(t)\right) - G + \frac{1}{2}C_d\rho_a u^2 S\right) \tag{32}$$

This equation can be solved for the velocity numerically, using, for example Matlab, once the gas temperature as a function of time is known.

3. SOLIDWORKS FLOW SIMULATION

A time-dependent flow simulation using SolidWorks is presented in this section. The simulation has been used to check the heat transfer model. At the same time, results are compared to real flight data to verify the simulation.

Geometry

The balloon geometry was obtained from the Ultramagic manufacturer. The geometry is a simplification since it is a smooth surface which does not include the shape of the gores (24 for the M series). The thickness of the envelope is 0.1 mm.

The main propane flame has been modeled as a cylindrical heat source. The total flame length is 5 m and the envelope is at a distance of 2.47 m. Based on observations these dimensions are reasonable (see Figure 12). The burner coil diameter is 235 mm. Accordingly, the cylinder in the model is 2.5 m long and has a 235 mm diameter.

Figure 12. Picture of the flame with the envelope as a reference

Figure 13 shows the model dimensions:

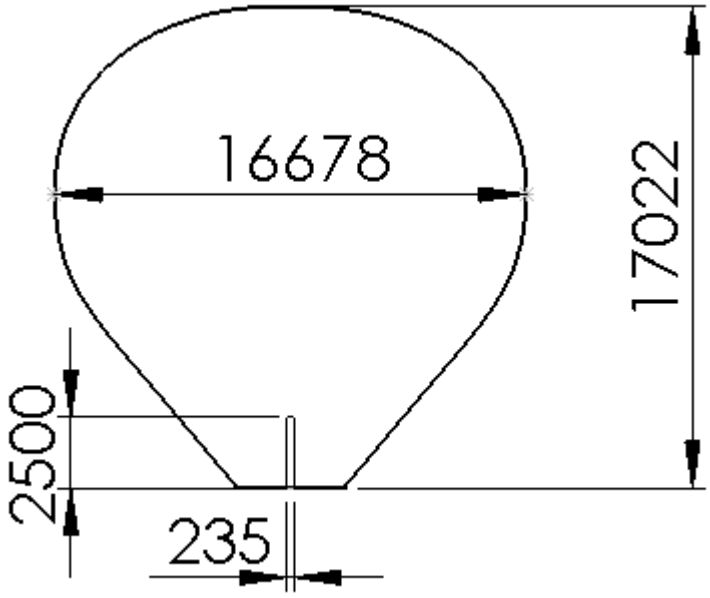

Figure 13. Basic dimensions (mm) of the balloon model used for the simulation

General settings

The solar radiation intensity has been set to 600 W/m^2.

The fluid inside the envelope is air and the properties for the envelope fabric have been set to a thermal conductivity of $k = 0.2\ W/mK$ and a density of 65 g/m^2 [8]. The emissivity has been set to $\varepsilon = 0.87$ for both the inner and outer surfaces.

Boundary conditions

There are two boundary conditions that need to be specified. First, there is the outer wall thermal condition. Since there is external convection, the parameters that needed to be input were the convection heat transfer coefficient, and the temperature of the external fluid. The convection coefficient is $h_{ext} = 3.37\ W/m^2K$ (see chapter 1), and the ambient temperature for this study is $T = 288.15\ K$.

Second, we need to set the boundary condition for the envelope opening at the bottom (or envelope mouth). It is a pressure opening set to ambient pressure $P = 101325\ Pa$ and temperature $T = 288.15\ K$. The temperature at the mouth is probably higher, around $310\ K$, but this does not affect the results.

Initial conditions

The initial temperature for the gas is set to $T_g = 373\ K$, which is the maximum continuous permitted temperature.

The initial temperature for the envelope is set to $T_s = 335\ K$, obtained from the heat transfer balance at the envelope (see chapter 0).

4. RESULTS

Heat Transfer Model

This section introduces the results from the heat transfer model. First a general case is considered, then a sensitivity analysis to atmospheric parameters is presented.

There are two unknown parameters: the envelope temperature T_s and the burner duty cycle k. The duty cycle is defined as the fraction of the total time that the burner has to be active in order to keep the balloon at a constant altitude, therefore at a constant gas temperature.

There are two equations that allow us to solve for T_s and k. There is the energy balance at the envelope:

$$Q_S(F_S, \alpha, A) + Q_{ab}(F_S, d, \alpha, A) + Q_{IRe}(\varepsilon_e, \varepsilon, \tau_a, A, T_e) + Q_{c,int}\left(T_s, T_g, h_{int}, A\right) + Q_r\left(T_s, T_g, \varepsilon_g, \varepsilon_{in}, A\right) - Q_{c,ext}(T_s, T_a, h_{ext}, A) - Q_{rad}(T_s, \varepsilon, A) = 0 \quad (33)$$

And the total energy balance:

$$Q_S + Q_{ab} + Q_{IRe} + Q_{IRa} - Q_{c,ext} - Q_{rad} + k(Q_{burner} - Q_o) = 0 \quad (34)$$

By solving the energy balance at the envelope we obtain the envelope temperature, which we consider to be uniform. The flow simulation shows that this is a good assumption. There is a 50 K overall variation in the surface but most of it is at the same temperature (see Figure 14).

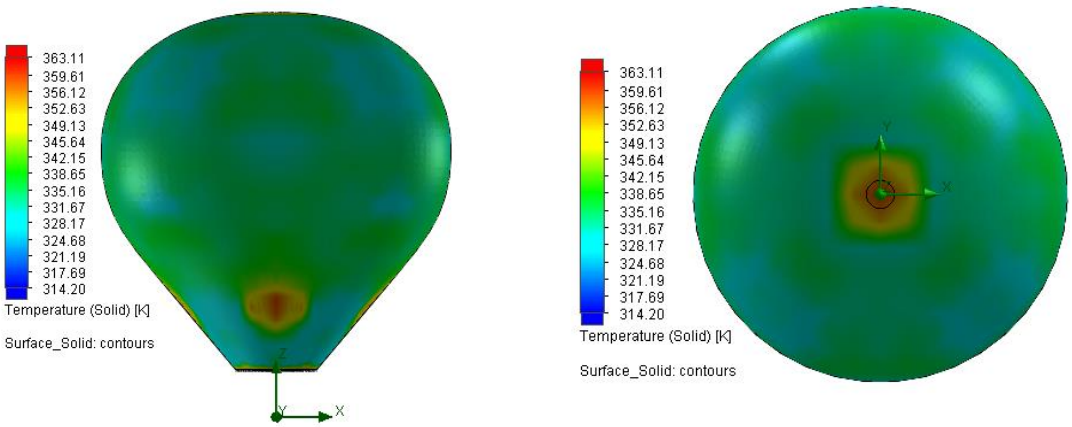

Figure 14. Flow simulation envelope temperature distribution (side and top views)

Once the envelope temperature is known, equation 34 can be solved to get the duty cycle.

General case

The baseline evaluation has incorporated standard sea level conditions, $T_a = 288\ K$. The internal temperature has been assumed to be the maximum continuous permitted temperature 373 K.

The Earth's surface emissivity ε_e is usually between 0.8 and 1. A value of 0.9 has been chosen.

It is assumed that it is a sunny day with clear sky, so the atmospheric transmissivity is set to $\tau_a = 0.65$ and the solar flux to 600 W/m^2 (see chapter 1). The albedo can go from 0.1 to 0.8 but for most surfaces is $d = 0.1$, which is the value selected here.

As for the fabric radiation properties, an average value has been taken for the absorptivity and the emissivity.

Table 2 summarizes the data needed to solve the problem and the conditions chosen for this study.

Variable	**Value**
Altitude	Sea Level
Ambient temperature	$T_a = 15℃ = 288.15\ K$
Gas temperature	$T_g = 100℃ = 373.15\ K$
External convection heat transfer coefficient	$h_{ext} = 3.4\ W/m^2K$
Internal convection heat transfer coefficient	$h_{int} = 16\ W/m^2K$
Earth's surface temperature	$T_e = 15℃ = 288.15\ K$
Atmosphere transmissivity	$\tau_a = 0.65$
Earth emissivity	$\varepsilon_e = 0.9$
Albedo	$d = 0.1$
Solar flux	$F_s = 600\ W/m^2$
Gas emissivity	$\varepsilon_g = 0.31$
Envelope absorptivity	$\alpha = 0.7$
Inner envelope emissivity	$\varepsilon_{in} = 0.87$
Outer envelope emissivity	$\varepsilon_{out} = 0.87$

Table 2. External conditions and fabric properties for the heat transfer analysis

For these conditions, the envelope temperature is calculated to be $\boldsymbol{T_s = 336.97\ K}$ and the duty cycle $\boldsymbol{k = 19.63\%}$.

Figure 15 shows the heat transfer modes in a hot air balloon and Figure 16 shows the heat inputs and losses.

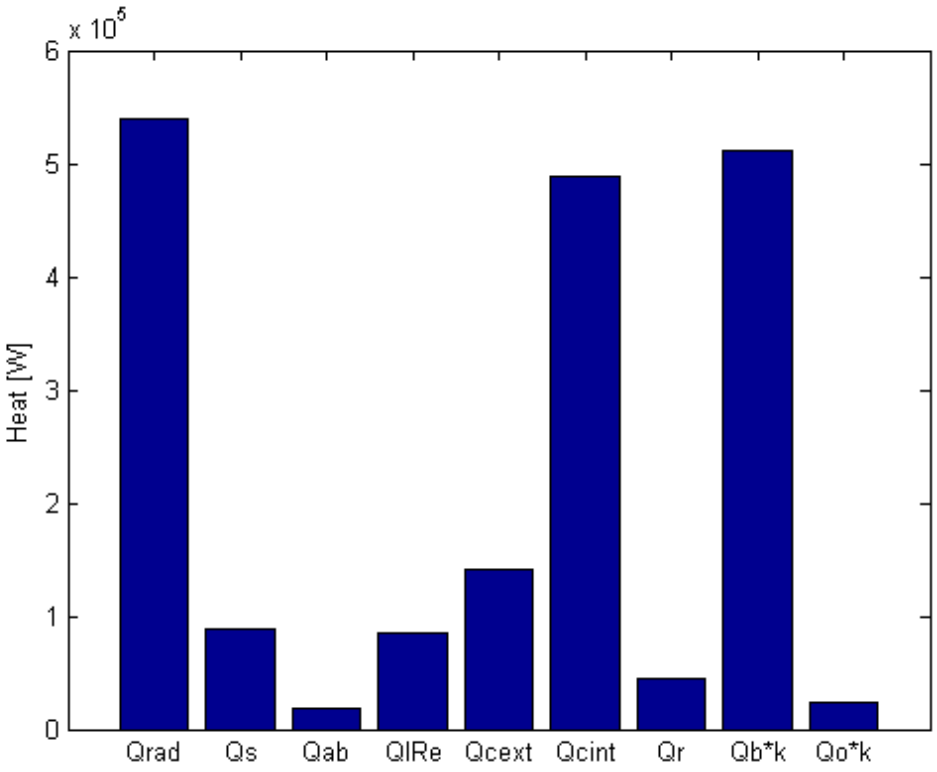

Figure 15. Heat transfer modes in a hot air balloon

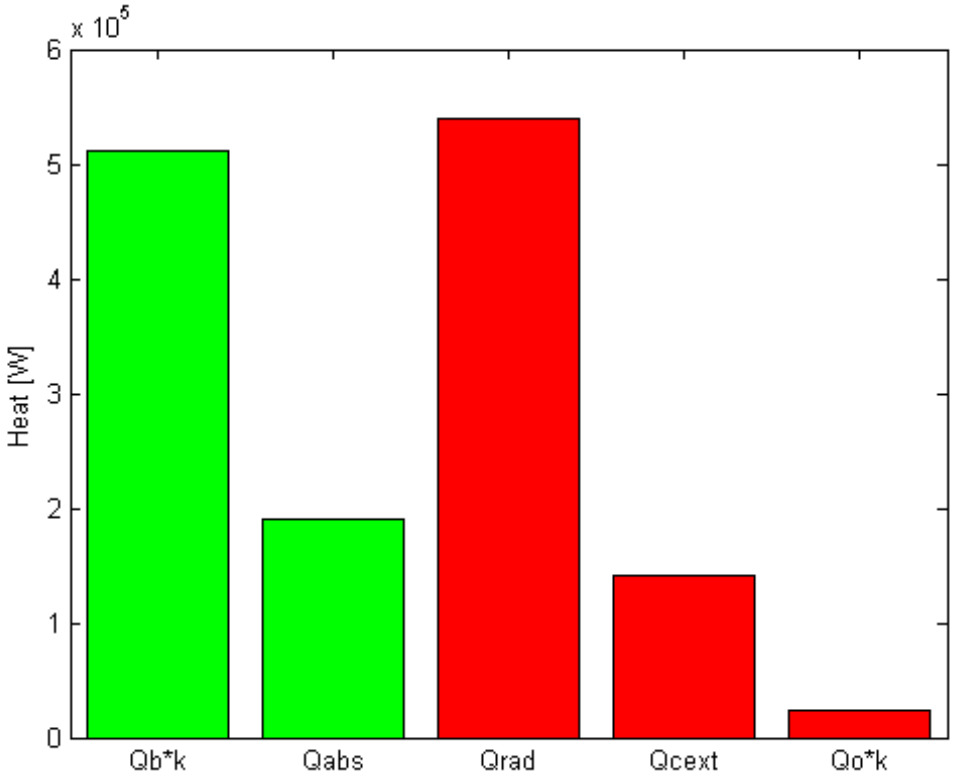

Figure 16. Hot air balloon heat inputs and heat losses

From Figure 15 and Figure 16 we can say that most of the heat losses are due to the emitted radiation from the envelope. They account for the 77% of the total. The losses from convection are much smaller but not negligible, accounting for another 20%. The remaining 3% is from the heat carried away by the overflow gases. When the balloon has vertical motion there is an increase in the convection coefficient and therefore an increase in convection heat loss, but it is still smaller than the radiative loss.

The percentage of heat that is absorbed by the envelope can change quite a lot, and therefore the burner operation time is very dependent on the flying conditions.

The radiation exchange from the envelope to the gas is negligible, and so are the errors associated with determining the gas emissivity.

Sensitivity

The overall fuel consumption (which relates to the thermal input balancing the thermal losses) depends on some parameters that can vary quite a lot. This section includes various plots that show fuel use dependency on atmospheric variables for different surface colors: black, white and silver. Black and white were chosen for its respectively high and low absorptivity, and silver because of its low emissivity. The plots also include a "general surface" with average values for emissivity and absorptivity. Table 3. Emissivity and absorptivity for different surface color gives the emissivity and absorptivity for different surface color:

Surface color	Emissivity	Absorptivity
Silver	0.7	0.48
White	0.88	0.53
Black	0.88	0.9
General	0.87	0.7

Table 3. Emissivity and absorptivity for different surface color

The atmospheric parameters that have been considered are the ambient temperature, the solar flux, the atmosphere transmissivity and the albedo coefficient.

Ambient temperature

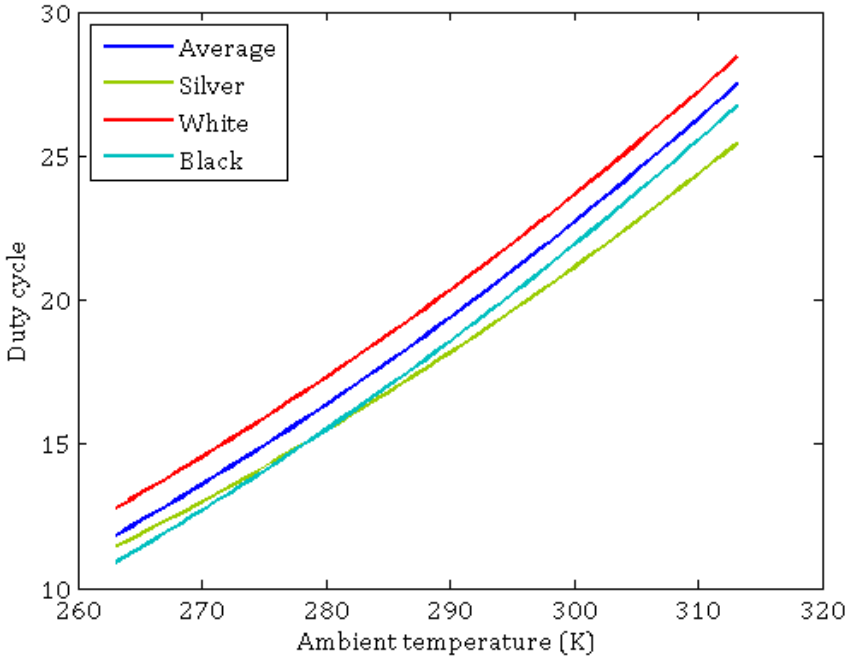

Figure 17. Duty cycle vs ambient temperature

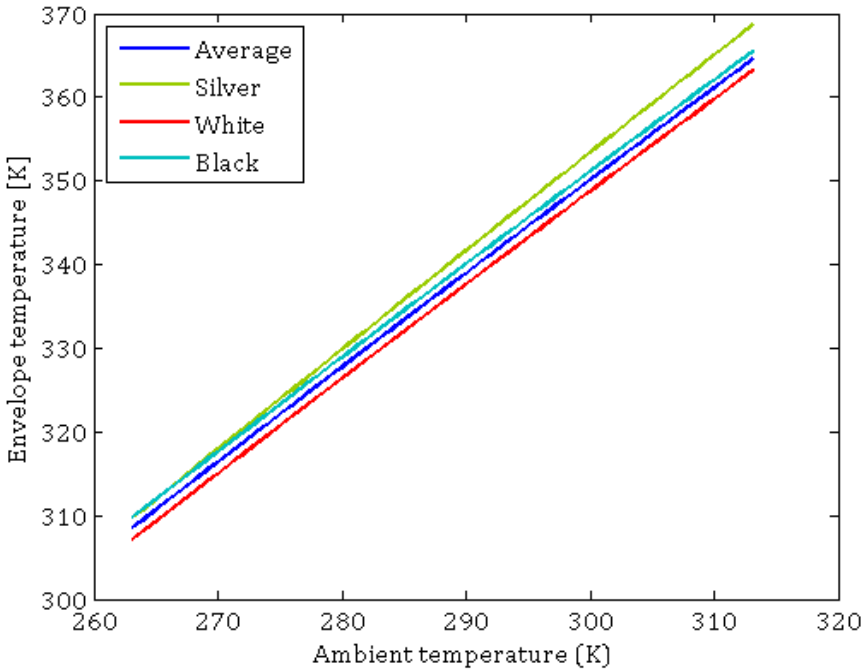

Figure 18. Envelope temperature vs ambient temperature

Albedo:

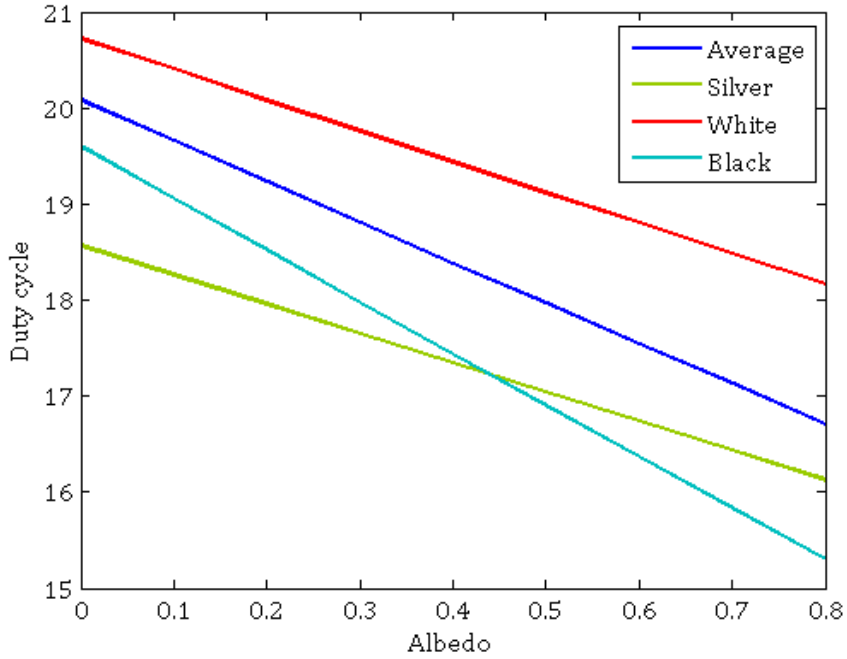

Figure 19. Duty cycle vs albedo coefficient

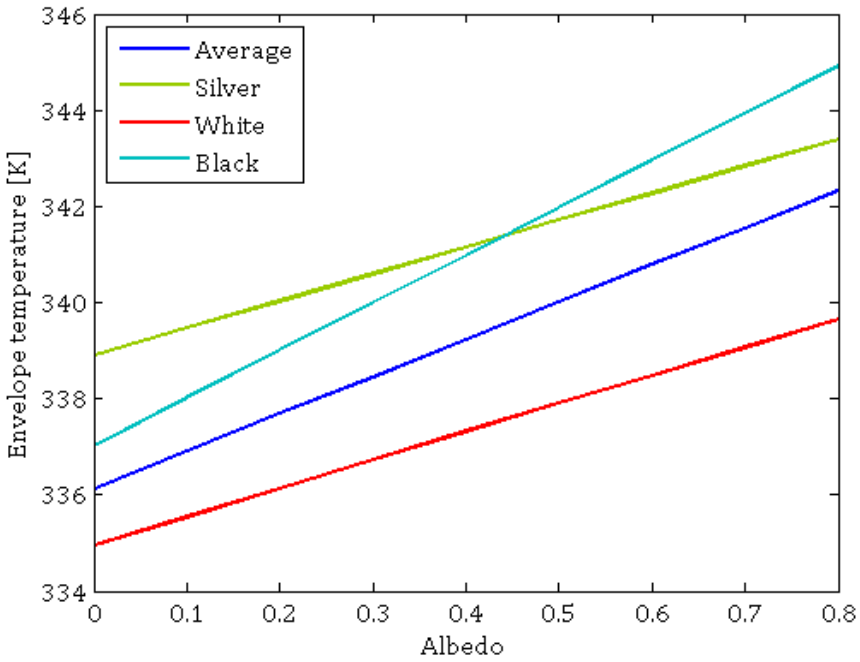

Figure 20. Envelope temperature vs albedo coefficient

Solar flux:

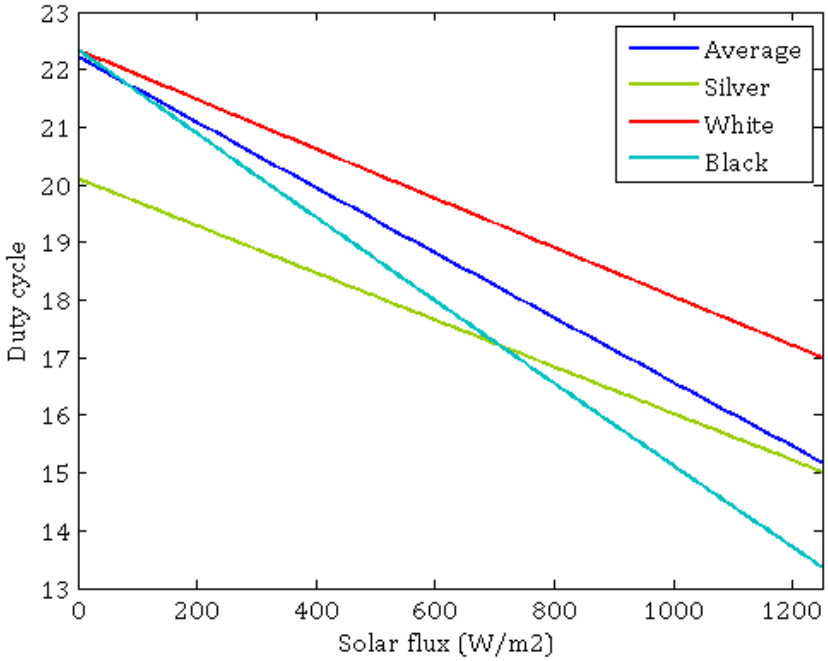

Figure 21. Duty cycle vs solar flux

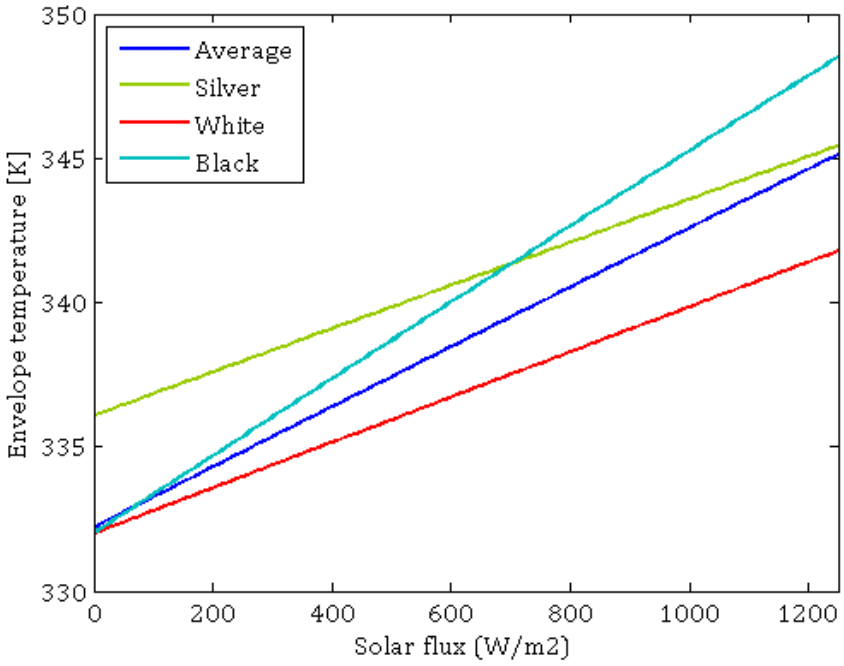

Figure 22. Envelope temperature vs solar flux

Atmospheric transmissivity:

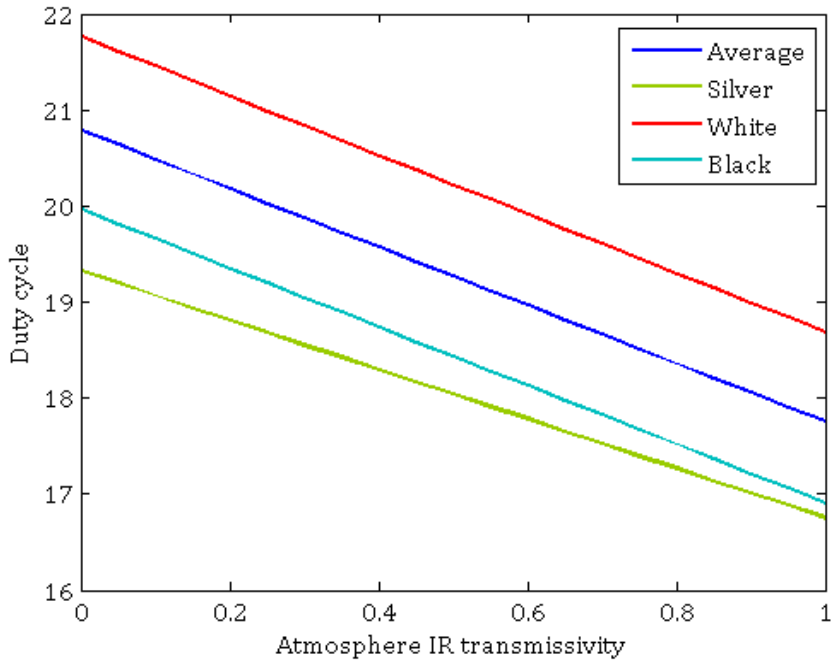

Figure 23. Duty cycle vs atmosphere IR transmissivity

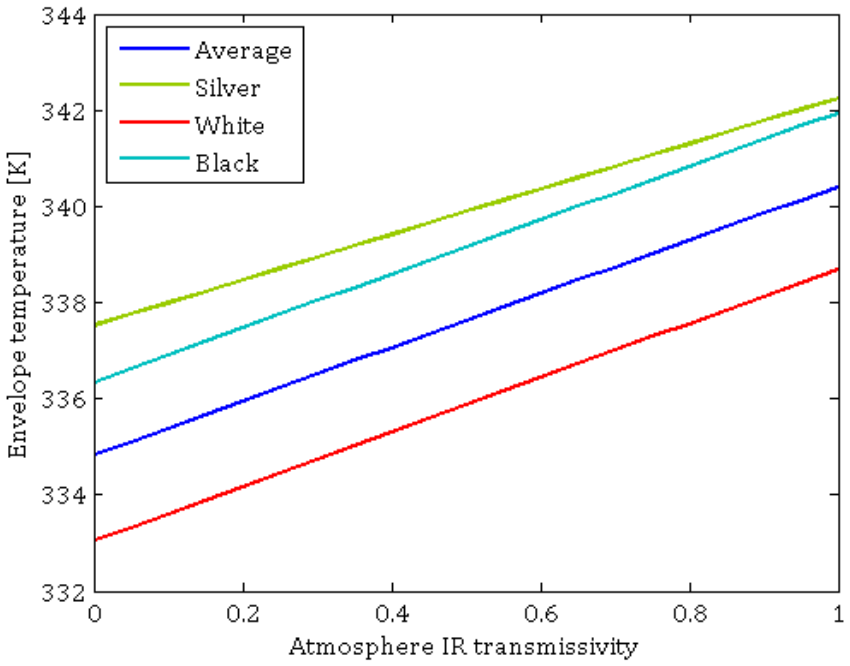

Figure 24. Envelope temperature vs atmosphere IR transmissivity

In all cases, fuel consumption is higher for the white fabric, but the envelope is at lower temperature which means longer life.

The black and silver fabrics are two extremes when considering fuel consumption. The black balloon has better performance for high solar flux (direct and reflected) and low ambient temperature ($T_a < 280\ K$), compared to the silver one. Also, a decrease in the atmosphere transmissivity has more effect on a black envelope. We can conclude that a black balloon is better for a sunny clear sky and a silver (reflective) balloon is better for a cloudy day.

The ambient temperature is the variable that most affects the fuel consumption, but it affects almost equally all fabric colors.

Flow Simulation

The flow simulation is used to verify the heat transfer model. This is done by activating the heat source, simulating the burner operation, to keep a constant temperature. Then results are compared to the analytically calculated burner duty cycle.

The initial condition for the fluid is a uniform temperature of $T_g = 373\ K$. In order to be closer to the real flow, it is required to let the gas mix. We let it cool down for 30 seconds until it comes to increasing isothermal layers (see Figure 25) and then we turn on the heat source until the average fluid temperature goes back to $T_g = 373\ K$. Next we let it cool down for 10 seconds and turn on the heat source for 3 seconds, which is the time required for the average temperature to go back to 373 K again. We repeat it another two times.

Finally, we let the temperature decrease for about 40 seconds, and from this temperature decrease with time we can calculate the descent rate and compare it to real flight data.

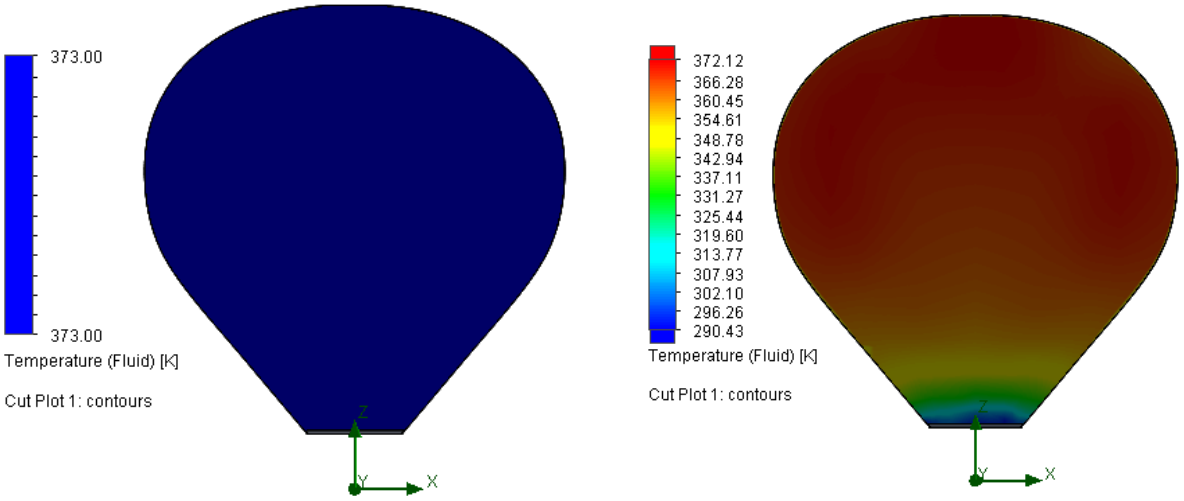

Figure 25. Gas temperature at simulation times t=0s (left) and t=30s (right)

Figure 26 shows the average gas temperature as a function of time. From point A ($t = 37\ s$) to point B ($t = 76s$) the heat source is active for $\Delta t_b = 3 \cdot 3 = 9\ s$. Then the duty cycle is $k = \Delta t_b / \Delta t = 0.23$. From the calculation we had obtained $k = 0.196$. It is a similar value, so it appears that there are no major errors in the analytical model.

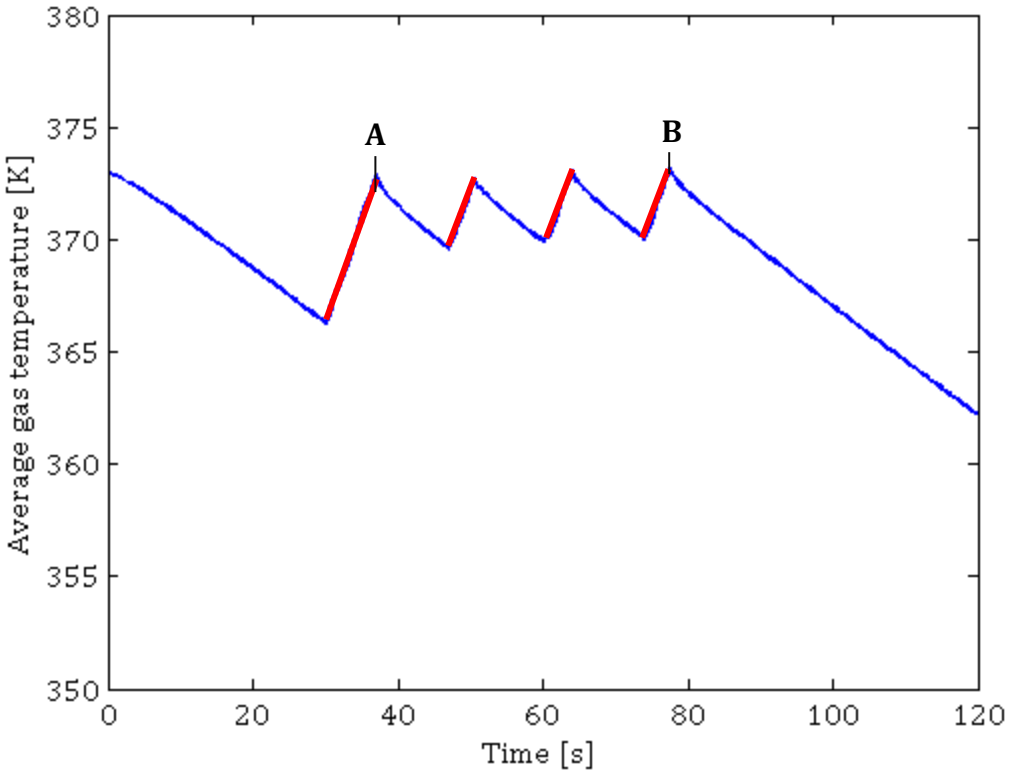

Figure 26. Average fluid temperature from the flow simulation with SolidWorks

From point B to the end of the simulation there is a decrease in temperature of $\Delta T_{coldfall} = 362.2 - 373.1 = -10.9\ K$ for a time period of $\Delta t_{coldfall} = 120 - 77.5 = 42.5\ s$. The temperature decrease rate is $-0.256\ K/s$, very similar to the experimental results from Aachen University [6] which give $-14.2\ K/min = -0.24\ K/s$.

Then we can say that the temperature as a function of time during descent is

$$T_g(t) = 373 - 0.256t \tag{35}$$

The equation for vertical motion is the following (see chapter 2):

$$\frac{du}{dt} = -\frac{1}{\left(V\rho_a\left(T_a/T_g(t)\right) + \frac{G}{g}\right)}\left(Vg\rho_a\left(1 - T_a/T_g(t)\right) - G + \frac{1}{2}C_d\rho_a u^2 S\right) \tag{36}$$

Solving the equation with $T_g(t)$ from the simulation we can obtain the descent velocity as a function of time (Figure 27), which matches real flight data.

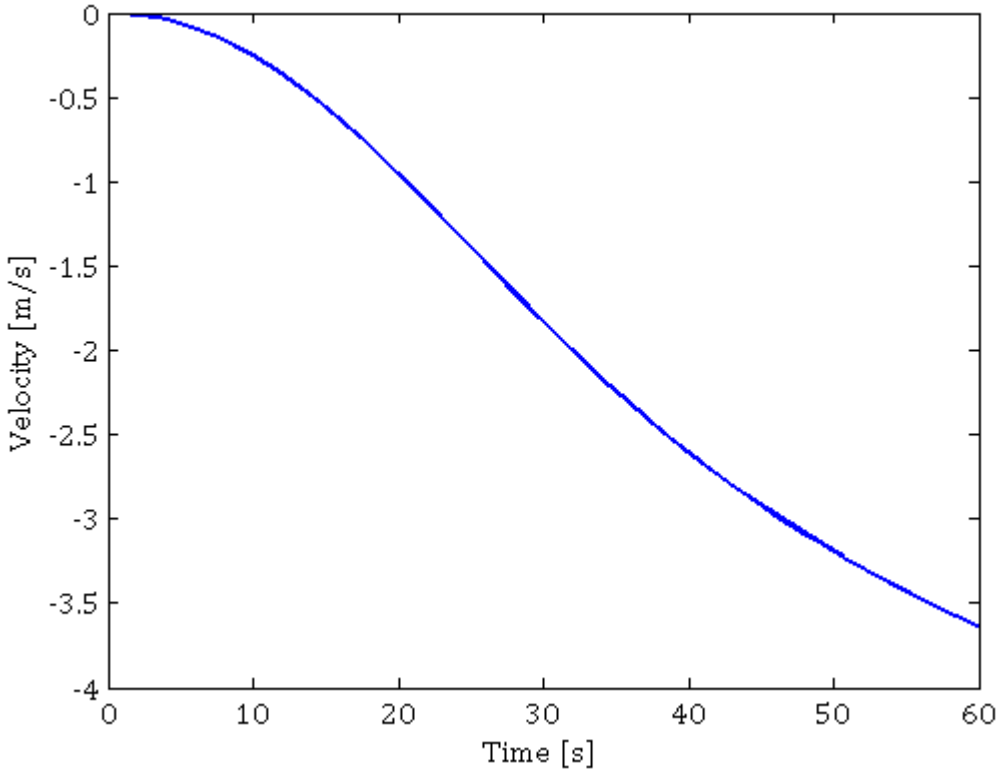

Figure 27. Descent rate as a function of time

We can integrate the velocity to get the change in altitude:

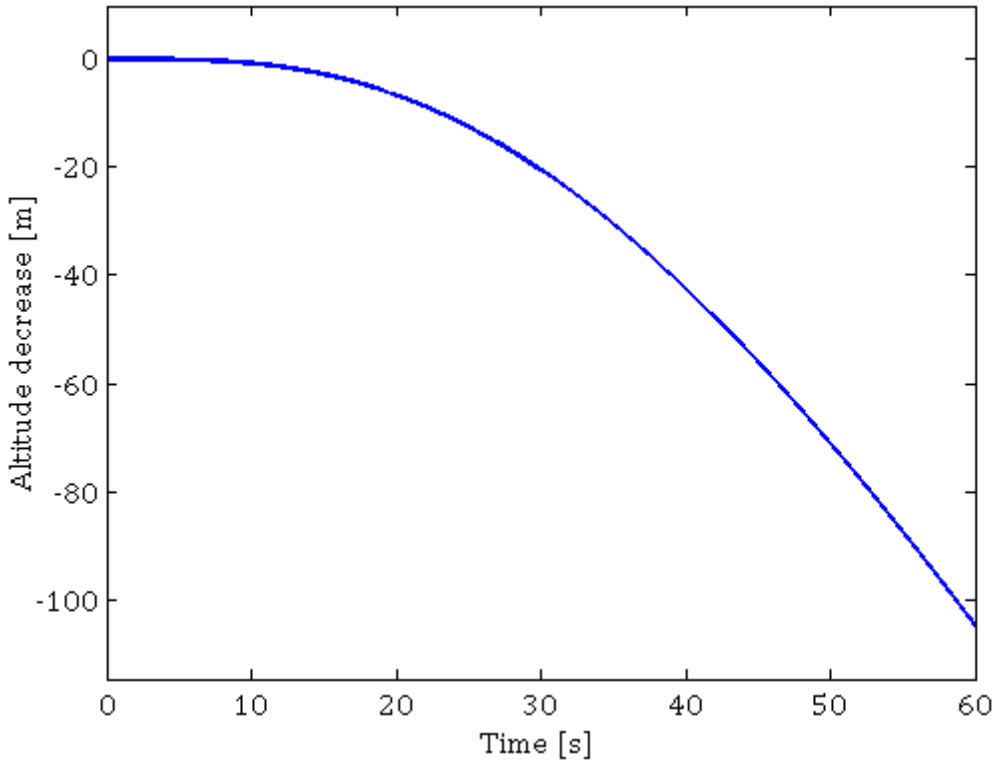

Actually the altitude would drop faster. The more velocity the higher the losses for convection are going to be and the faster the temperature is going to decrease.

Figure 28 shows the change in temperature distribution when the burner is active and few seconds after that. For more detail see Appendix I.

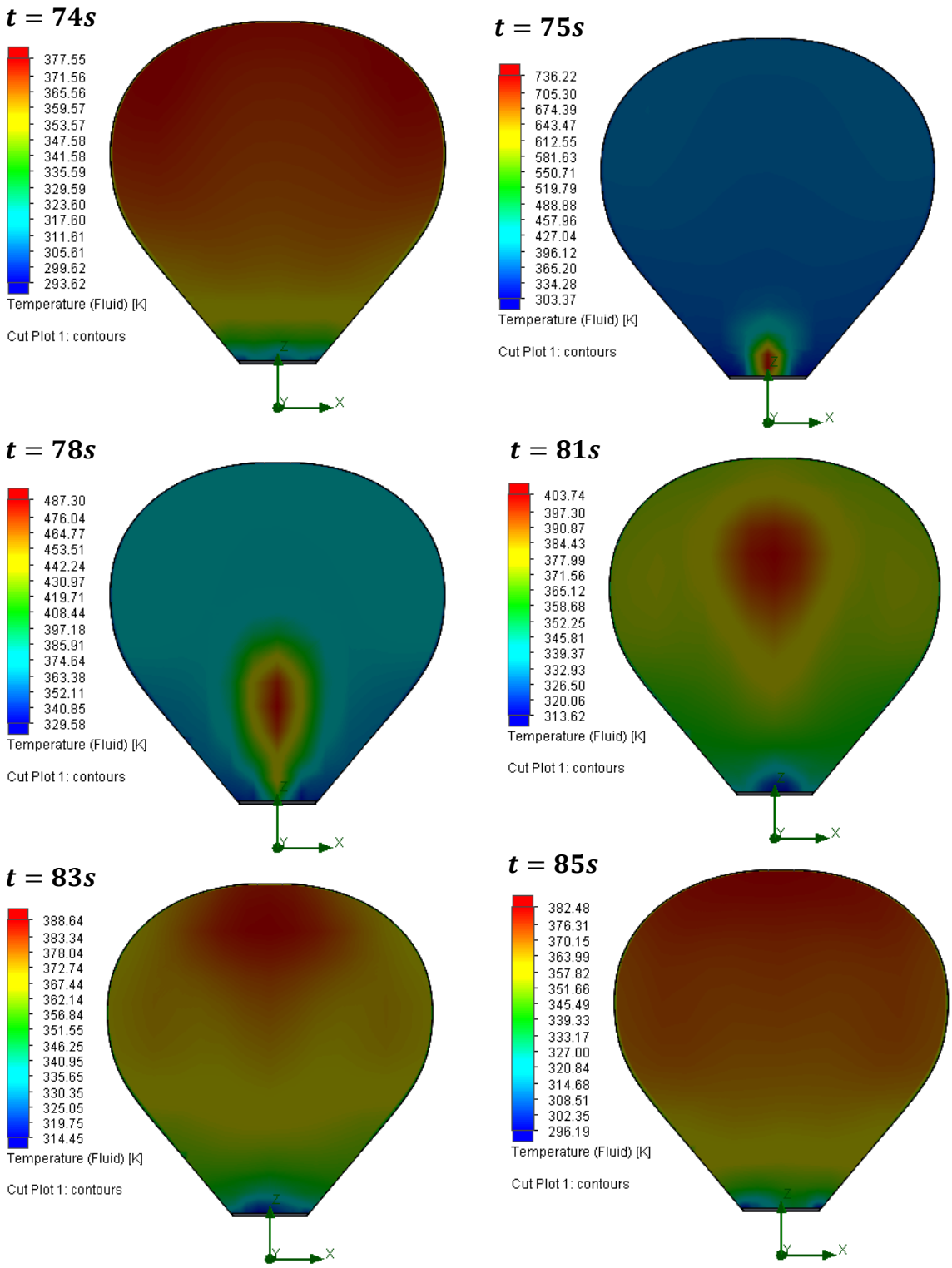

Figure 28. Gas temperature during burner activity (second 74 to second 77.5)

5. CONCLUSIONS

A heat transfer model was developed to calculate the fuel consumption in a hot air balloon. The model was then evaluated by varying typical parameters to determine optimal designs and important parameters. Since some parameters are difficult to assess, a flow simulation was used to verify the analytical results and to give more insight on the thermal distribution.

Results from the flow simulation show that there are no major errors in the analytical model since burner operation times agree when attempting to maintain a constant altitude. The gas temperature decreases at a rate of $-0.256\ K/s$ when there is no burner activity, and it increases at a rate of $+1\ K/s$ when the pilot operates the burner. The simulation results also show that the assumption of uniform temperature in the envelope is correct, and that after approximately 10 seconds after burner operation the gas comes to increasing isothermal layers. The temperature decrease rate matches the experimental one from Aachen University, and the vertical speed agrees with real flight data, indicating that the simulation can be trusted.

The analytical results for the general typical case show that most of the heat losses are due to the emitted radiation from the envelope (more than 70%), the losses from natural convection account for around 20% of the total, and the mouth outflow losses are relatively small. From the sensitivity analysis, we get that the burner duty cycle (to keep the balloon at a constant altitude) at different atmospheric conditions can be from 10% to 28%. We can conclude that the ambient temperature is the variable that most affects the fuel consumption, increasing with increasing ambient temperature. Unfortunately, ambient

temperature is not a controllable parameter so its effects can only be predicted but not mitigated. A black fabric is more economical in terms of fuel for a sunny clear sky day, and a silver balloon is better for a cloudy day. Light colors, which have low absorptivity, have the worst performance, as expected, but the envelope is at lower temperature which can mean longer life for the fabric.

Future work

The performance model presented here is very simple. With an improved model the altitude can be related to the gas temperature more accurately. We already know that the decrease rate in coldfall is $-0.256\,K/s$ and that 1 second of burner operation is needed to increase the temperature by $1\,K$, so it would be possible to approximate the fuel needed for a planned flight. This is very critical for long distance flights where maximum payload is a limitation to decide how much fuel to carry in the balloon.

An additional opportunity for future work is to determine if there are methods to heat the enclosed gas but prevent that heat from reaching the inner envelope surface. This would provide low density gas with a low temperature envelope to reduce losses. Such a design might require some careful fluid mechanics study of the entrained gases during combustion and their eventual flow patterns in the balloon.

Finally, a last aspect of future work is to evaluate more completely the combustion characteristics of the burner to ensure that it has the combustion efficiency expected.

REFERENCES

[1] F. Kreith, "Numerical Prediction of the Performance of High Altitude Balloons," no. February, 1974.

[2] F. Kreith, "Thermal Design of High-Altitude Balloons and Instrument Packages," *J. Heat Transfer*, 1970.

[3] L. A. Carlson and W. J. Hornt, "New Thermal and Trajectory Model for High-Altitude Balloons," vol. 20, no. 6, pp. 500–507, 1982.

[4] K. Stefan, "Performance Theory for Hot Air Balloons," *J. Aircr.*, vol. 16, no. 8, pp. 539–542, Aug. 1979.

[5] W. Hallmann and U. Herrmann, "Thermodynamics of Balloon," in *International Symposium on Hot Air Aerostatic Vehicle Technology*, 1991.

[6] W. Hallmann and U. Herrmann, "Experimentally determined Temperature Profile in a Hot Air Balloon," in *International Symposium on Hot Air Aerostatic Vehicle Technology*.

[7] R. Röder, U. Rönna, and F. Suttrop, "Measurement of velocity distribution and gas composition in the envelope of a flying hot air balloon," in *International Symposium on Hot Air Aerostatic Vehicle Technology*, 1991.

[8] W. Hallmann and U. Herrmann, "Energy Losses, Porosity, Strength and Stretch Behavior of Hot Air Balloon Fabrics Subject to Temperature Loads and Ultraviolet Radiation," in *International Symposium on Hot Air Aerostatic Vehicle Technology*, 1991.

[9] H. a. Becker and S. Yamazaki, "Entrainment, momentum flux and temperature in vertical free turbulent diffusion flames," *Combust. Flame*, vol. 33, pp. 123–149, Jan. 1978.

[10] J. Jones and J. Wu, "Performance model for reversible fluid balloons," in *AIAA*, 1995.

[11] A. Campo, "Correlation equation for laminar and turbulent natual-convection from spheres," *Warme Und Stoffubertragung -- Thermo Fluid Dyn.*, vol. 13, no. 1–2, pp. 93–96, 1980.

[12] "[1] British Standard BS845 : Part 1 : 1987 for assessment of thermal performance," no. 1. .

[13] A. Gillespie, “Land Surface Emissivity,” in *Encyclopedia of Remote Sensing*, E. G. Njoku, Ed. New York, NY: Springer New York, 2014.

[14] D. F. Al Riza, S. I. U. H. Gilani, and M. S. Aris, “Hourly Solar Radiation Estimation Using Ambient Temperature and Relative Humidity Data,” *Int. J. Environ. Sci. Dev.*, vol. 2, no. 3, pp. 188–193, 2011.

[15] T. Colonius and D. Appelö, “Computational Modeling and Experiments of Natural Convection for a Titan Montgolfiere,” no. x, pp. 1–16, 2016.

Appendix I. SIMULATION RESULTS

$t = 0\ s$

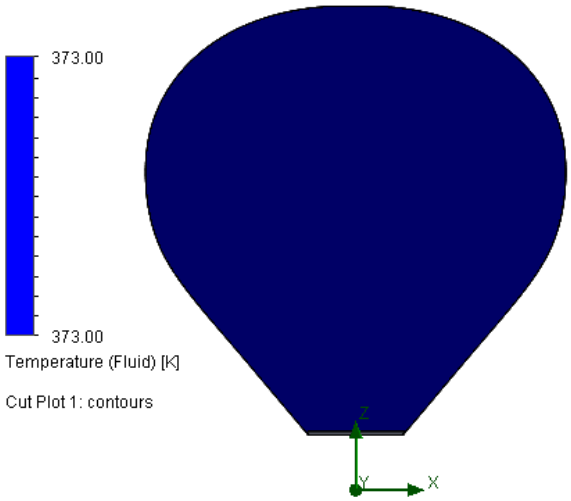

$t = 30\ s$

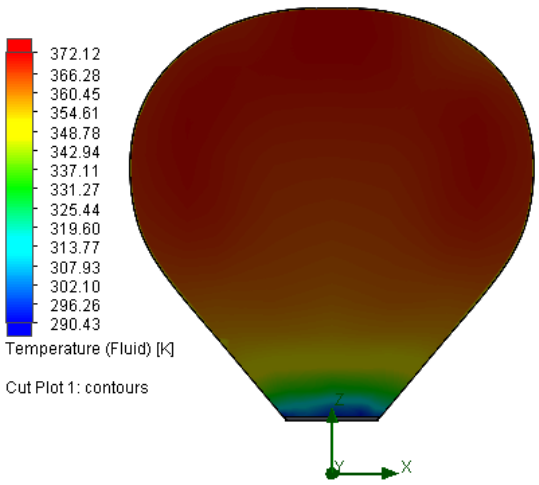

$t = 74\ s$

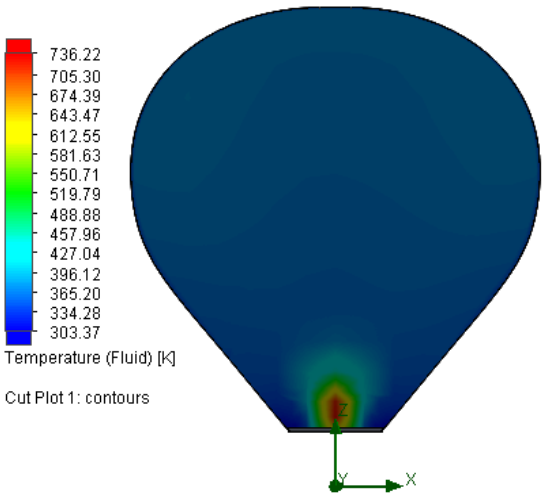

$t = 75\ s$

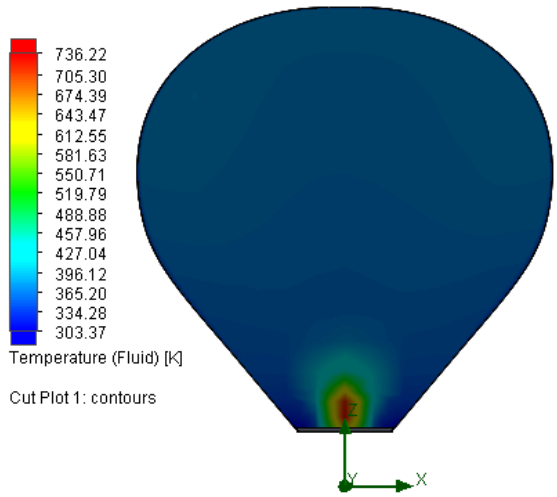

$t = 76\ s$

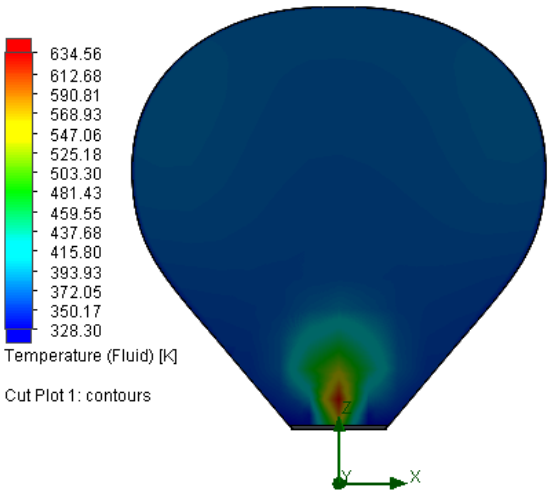

$t = 77\ s$

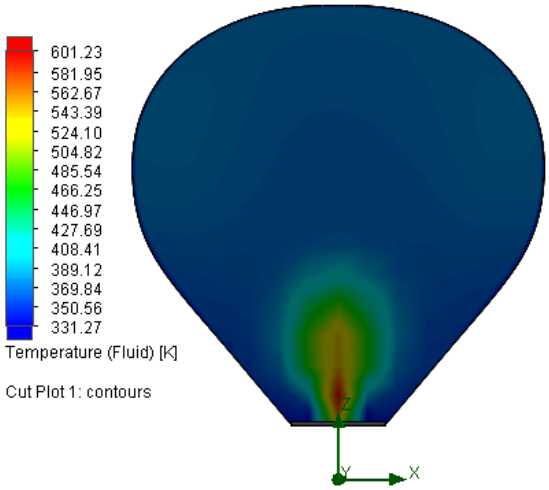

$t = 78\ s$

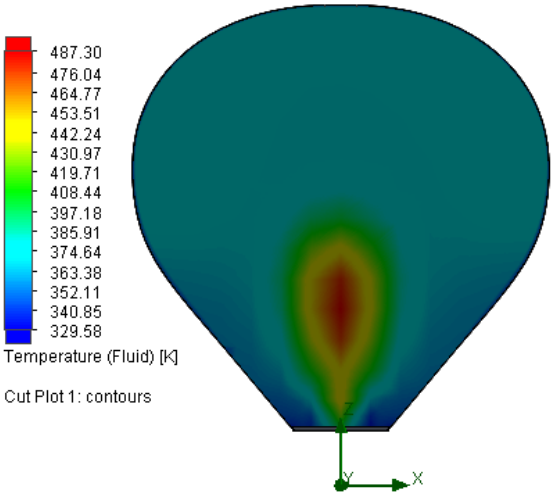

$t = 79\ s$

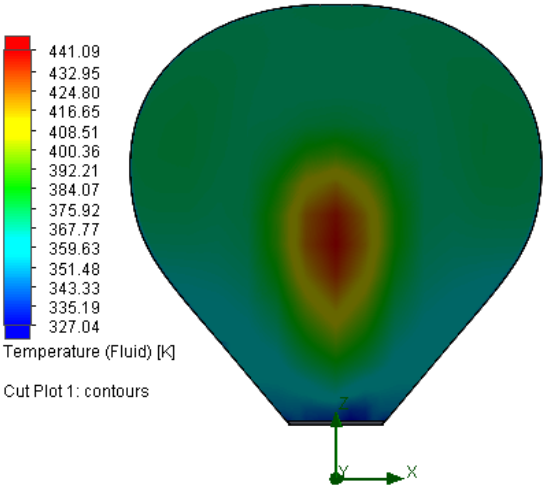

$t = 80s$

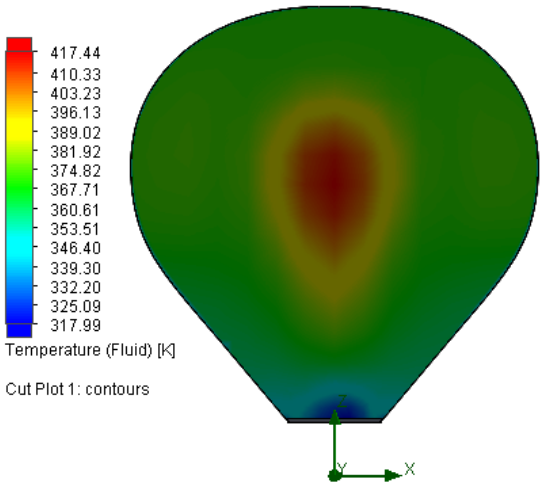

$t = 81\ s$

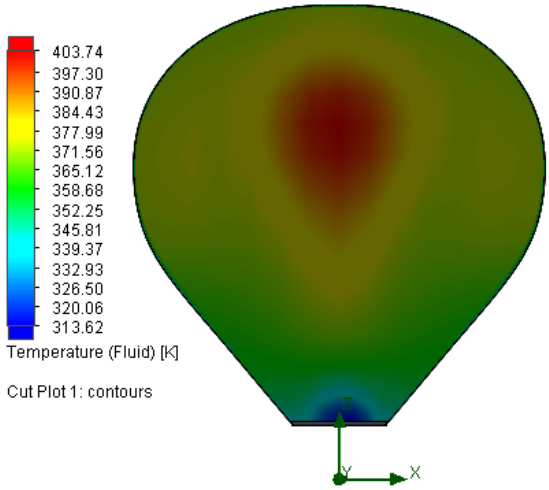

$t = 82\ s$

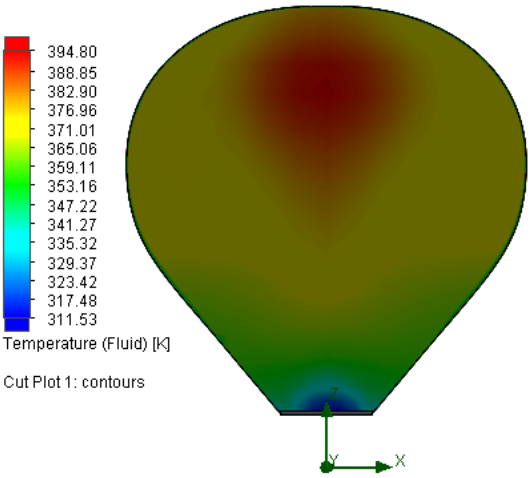

$t = 83\ s$

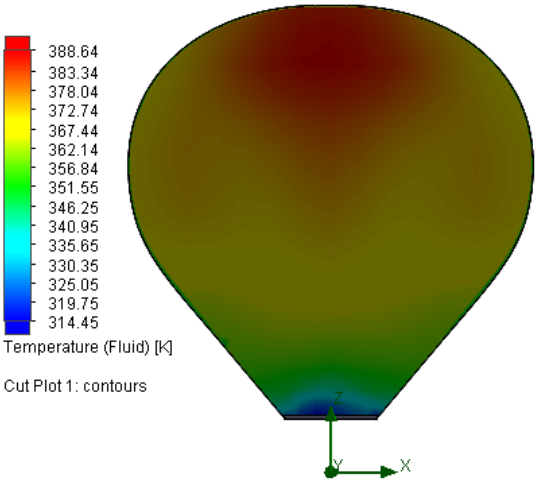

$t = 84\ s$

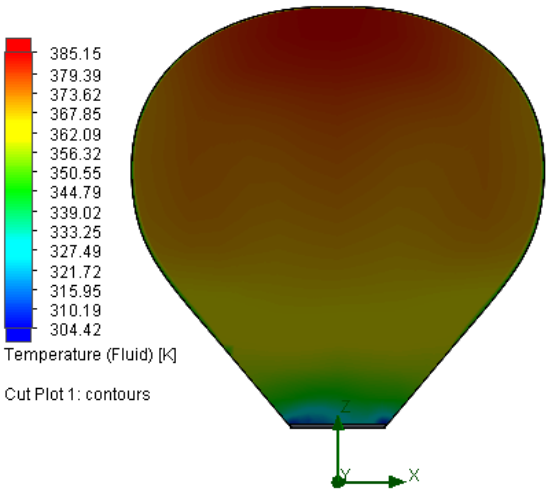

$t = 85\ s$

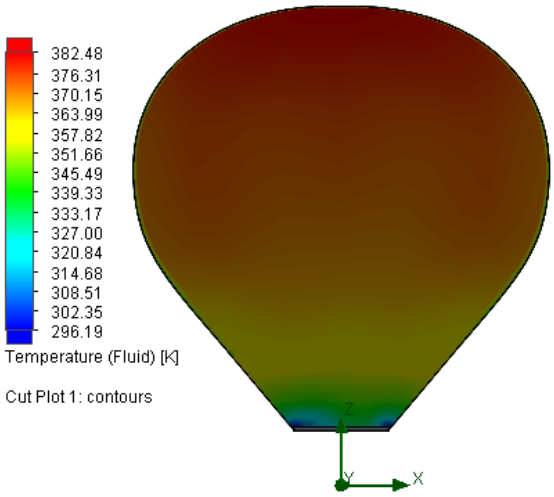

$t = 86\ s$

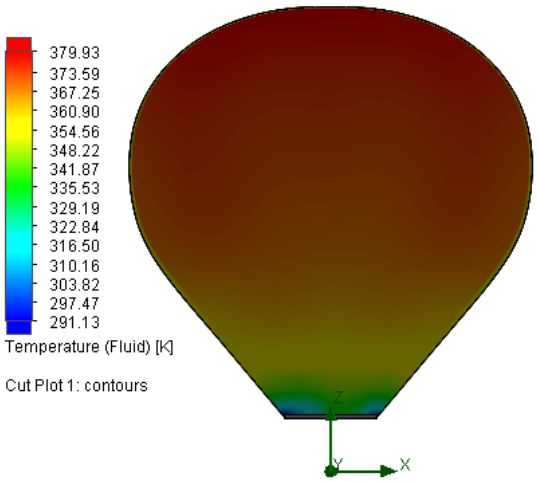

$t = 100\ s$

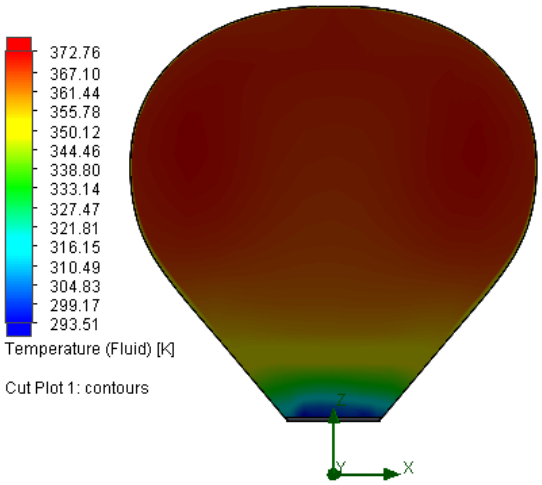

Appendix II. MATLAB SCRIPT

Heat transfer balance

```
%%%%%%%%%DATA%%%%%%%
sigma=5.67e-8; %[W/m2K4] Stephan-Boltzmann constant
R=287; %[J/kgK] Air gas constant
g=9.81; %[m/s2]

%Atmosphere
Ta=15+273.15; %[K] Ambient temperature
P=101325; %[Pa] Ambient pressure
rhoa=P./(R*Ta); % Ambient density
Fs=600; %[W/m2] Solar flux
tau_a=0.65; % Infrarred transmissivity of the atmosphere


%Earth surface
Te=Ta; %[K] Earth surface temperature
eps_e=0.9; % Earth surface emissivity
d=0.1; % Albedo

%Balloon envelope
V=2200; %[m3] Gas volume
A=847; %[m2] Surface area for M77 V=2200m3
eps=0.87; alpha=0.7; %Emissivity and absorptivity of outer
surface
eps_in=0.87; % Emissivity of the inner side of the fabric

%Internal gas
Tg=373; % [K]Emissivity
eps_g=0.45;

%Envelope temperature
[Ts]=EnvelopeT(sigma,R,Ta,P,Fs,tau_a,Te,eps_e,d,A,eps,alpha,eps_
in,Tg,eps_g);
fprintf('Envelope temperature: %.2f K \n',Ts);

%Burner
Qburner=(3255e3)*0.8; %[W] Burner heat input
```

```
%%%%%%%%%HEAT TRANSFER MODES%%%%%%%
%%EMITTED RADIATION FROM THE ENVELOPE
Qrad=eps*sigma*A*Ts^4;


%%EXTERNAL CONVECTION
h_ext=3.4; %[W/m2K] External convection coefficient
Qc_ext=h_ext*A*(Ts-Ta);

%%SOLAR RADIATION
%Solar direct radiation
Qs=Fs*alpha*A/4;

%Reflected solar radiation (albedo)
Qab=Fs*d*alpha*A/2;

%%INFRARRED RADIATION FROM THE EARTH
%Earth IR radiation
QIRe=eps_e*eps*tau_a*sigma*(A/2)*Te^4;

%%RADIATION GAS-ENVELOPE
f=1/((1-eps_g)/eps_g+1+(1-eps_in)/eps_in);
Qr=sigma*A*f*(eps_g*Tg^4-eps_in*Ts^4);

%%INTERNAL CONVECTION
h_int=16; %[W/m2K] Internal convection coefficient
Qc_int=h_int*A*(Tg-Ts);

%MOUTH OUTFLOW
cpair=1.011; %[J/gK]
m_dot=1356; %[g/s] Mass flow at the mouth
Qo=m_dot*cpair*(Tg-Ta);

%HEAT BALANCE
duty=@(k) Qs+Qab+QIRe+Qburner*k-Qc_ext-Qrad-Qo*k;

k=fzero(duty,0.1);

duty_cycle=k*100;
fprintf('Duty cycle: %.2f \n',duty_cycle);
```

Envelope temperature function

```
function [Ts] =
EnvelopeT(sigma,R,Ta,P,Fs,tau_a,Te,eps_e,d,A,eps,alpha,eps_in,Tg
,eps_g)

     %%%%%%%%%HEAT TRANSFER MODES%%%%%%%
     %%EMITTED RADIATION FROM THE ENVELOPE
     Qrad=@(Ts) eps*sigma*A*Ts^4;

     %%EXTERNAL CONVECTION
     h_ext=3.4; %[W/m2K]
     Qc_ext=@(Ts) h_ext*A*(Ts-Ta);

     %%SOLAR RADIATION
     %Solar direct radiation
     Qs=Fs*alpha*A/4;

     %Reflected solar radiation (albedo)
     Qab=Fs*d*alpha*A/2;

     %%INFRARRED RADIATION FROM EARTH
     %Earth IR radiation
     QIRe=eps_e*eps*tau_a*sigma*(A/2)*Te^4;

     %%RADIATION GAS-ENVELOPE
     Qr=sigma*A*f*(eps_g*Tg^4-eps_in*Ts^4);
     Qr=@(Ts) sigma*A*f*(eps_g*Tg^4-eps_in*Ts^4);

     %%INTERNAL CONVECTION
     h_int=16; %[W/m2K]
     Qc_int=@(Ts) h_int*A*(Tg-Ts);

     %%%%%%HEAT BALANCE%%%%%%%
     envelope=@(Ts) Qs+Qab+QIRe+Qc_int(Ts)+Qr(Ts)-Qc_ext(Ts)-
     Qrad(Ts);

     Ts=fzero(envelope,Ta);
end
```

Vertical motion

```
syms v(t)

[t,v] = ode45(@verticalmotion_velocity,[0,60],0)

function dvdt=verticalmotion_velocity(t,v)

     g=9.81; %[m/s2]
     Ta=288.15; %[K] Ambient temperature
     rho=1.225; %[kg/m3] Ambient density


     %Balloon parameters
     V=2200; %[m3] Gas volume
     r=16.67/2; %[m] Radius at the equator
     S=pi*r^2; %[m2] Balloon cross-sectional area
     Cd=0.43; %Drag coefficient
     M=613; %[kg]
     G=g*M; %[N] Weight for L=G at sea level and Tg=373 K


     Tg=373-0.256*t; %[K] Gas temperature as a function of time

     L=V*g*rho*(1-Ta./Tg);
     B=Cd*0.5*rho*S;
     m=(rho*(Ta./Tg)*V+M);

     if L>G
          dvdt=(L-G-B*(v^2))./m;
     elseif L<G
          dvdt=(L-G+B*(v^2))./m;
     end
end
```